ÉCOLE DE TECHNOLOGIE SUPÉRIEURE
UNIVERSITÉ DU QUÉBEC

THESIS PRESENTED TO
ÉCOLE DE TECHNOLOGIE SUPÉRIEURE

IN PARTIAL FULLFILMENT OF THE REQUIREMENTS FOR
THE DEGREE OF
MASTER OF ENGINEERING
M. ENG.

BY
ELZAYAT, Ahmed

DESIGN AND REALISATION OF FILTERS ON MHMIC AND MMIC FABRICATION PROCESSES FOR DUPLEXERS REALISATION

MONTREAL, MARCH 7, 2008

THIS THESIS HAS BEEN EVALUATED

BY THE FOLLOWING BOARD OF EXAMINERS:

M. Ammar B. Kouki, director
Department of electrical engineering at the École de technologie supérieure

M. Christian Gargour, jury president
Department of electrical engineering at the École de technologie supérieure

Vahé Nerguizian, jury member
Department of electrical engineering at the École de technologie supérieure

THIS THESIS HAS BEEN PRESENTED AND DEFENDED

ON FEBRUARY, 6, 2008

AT ÉCOLE DE TECHNOLOGIE SUPÉRIEURE

ACKNOWLEDGEMENTS

I would like first of all to thank, my mother for nourishing the sense of wonder that god blessed me with since I started to read about physics and science in general at a quite young age, my father for his moral and financial support, and my wife for her support and understanding.

On the professional level I would like to thank Prof. Ammar Kouki for his guidance and encouragement through my work and for his effort in elucidating some of the most difficult concepts in electromagnetics in a clear concise way. Here I have to admit that his courses in the École de Technologie Supérieure, and I have attended all of them, were particularly inspiring.

Finally, I would like to extend my thanks to my colleagues in the LACIME laboratory for the enriching discussions both on the scientific and personal levels.

Above all I would like to thank Allah for giving me the patience and the perseverance to complete the work related to this dissertation through difficult times in my life.

CONCEPTION ET RÉALISATION DE FILTRES SUR MHMIC MMIC ET PROCÉDÉS DE FABRICATION POUR LA RÉALISATION DE DEPLEXEURS

ELZAYAT, Ahmed

RÉSUMÉ

Dans l'environnement actuel des télécommunications, les terminaux multi-modes multi-bandes sont couramment utilisés dans les systèmes de communications modernes. Ces terminaux intègrent plusieurs « front-ends » radiofréquences (RF), chacun pour une bande de fréquences, dont le fonctionnement nécessite des filtres ou duplexeurs RF. En plus, les filtres RF sont de tailles relativement importantes par rapport à d'autres composants RF. Par conséquent, les filtres et les duplexeurs occupent une partie de plus en plus grande dans les émetteurs-récepteurs modernes. Ceci a conduit la communauté scientifique à consacrer plus d'efforts à la miniaturisation des filtres radiofréquences.

Le présent travail s'inscrit dans ce contexte, dans un effort visant à mettre au point des filtres et des duplexeurs miniaturisés ayant de faibles pertes et une haute isolation. Ce mémoire présente une topologie de filtres / duplexeurs miniaturisés basée sur une technique de miniaturisation topologique en utilisant l'analyse et la conception assistées par ordinateur. Les filtres conçus dans ce travail s'adapte bien à des procédés de fabrication en technologies planaires. Telles que "Monolithic Hybrid Microwave Integrated Circuit (MHMIC)" et "Monolithic Microwave Integrated Circuit (MMIC)". Ces procédés ont été choisit à cause de leurs caractéristiques de miniaturisation et d'intégration. Les filtres obtenus montrent une réduction significative de taille par rapport à l'état de l'art. La technique de miniaturisation utilisée peut être combinée avec les technologies de fabrication multicouches et d'autres techniques avancées de fabrication pour potentiellement aboutir à des filtres / duplexeurs de tailles raisonnables pour une intégration monolithiques.

DESIGN AND REALISATION OF FILTERS ON MHMIC AND MMIC FABRICATION PROCESSES FOR DUPLEXERS REALISATION

ELZAYAT, Ahmed

ABSTRACT

In the current telecommunication environment, multimode multiband terminals are common place in transceivers architectures. These terminals integrate several radio frequency front-ends each for a different radio frequency band. Proper operation requires a separate radio frequency filter or duplexer for each band. In addition to this, filters are relatively large in size compared to other front-end components. Consequently, filters and duplexers occupy an increasing portion of modern radio frequency transceivers' real-estate. This has led the research community to dedicate more effort to filter miniaturisation techniques.

This work subscribes to this context in an effort to develop miniaturised filters and duplexers with low losses and high isolation. This thesis presents a miniaturised topology based on a topological miniaturisation technique using computer aided design and analysis. The filters designed in this work are suitable for manufacturing on any planar fabrication technology such as Monolithic Hybrid Microwave Integrated Circuit (MHMIC) and Monolithic Microwave Integrated Circuit (MMIC). These specific processes were selected and used for fabrication because of their high miniaturisation and integration features. The realised filters show a significant reduction in size compared to the current state of the art. The proposed miniaturization technique, combined with multilayer fabrication technologies and other fabrication advancements, can potentially lead to filters and duplexers of reasonable sizes for monolithic integration.

TABLE OF CONTENTS

LIST OF TABLES

Page

LIST OF FIGURES

Page

LIST OF ACRONYMS

ADS	Advanced Design System
BAW	Bulk Acoustic Wave
BiCMOS	Bipolar Complementary Metal Oxide Transistor
CPW	Coplanar Wave Guide
FDD	Frequency Division Duplex
GaAs	Gallium Arsenide
GSM	Global System for Mobile communication
HBT	Hetero-junction Bipolar Transistor
LNA	Low Noise Amplifier
LTCC	Low Temperature Co-fired Ceramics
MHMIC	Microwave Hybrid Monolithic Integrated Circuit
MMIC	Microwave Monolithic Integrated Circuit
MS	MicroStrip
PA	Power Amplifier
pHEMT	pseudomorphic High Electron Mobility Transistor
RF	Radio Frequency
SAW	Surface Acoustic Wave
TDD	Time Division Duplex
UMTS	Universal Mobile Telecommunication System
WCDMA	Wide band Code Division Multiple Access

INTRODUCTION

Motivation and Background

On the road to ubiquitous connectivity, the wireless telecommunication industry is witnessing an unprecedented demand for multi-mode multi-service wireless user terminals. As manufacturers try to fulfill these demands, major challenges arise causing an ever increasing difficulty in this endeavour. While manufacturers are increasing the number of circuits integrated into a terminal, they are faced with the insatiable demand of the consumer to have lighter, smaller, and cheaper terminals.

On the other side, the coexistence of a multitude of wireless standards necessitates excellent management of the radio frequency resources and isolation between different radio frequency bands.

Radio frequency filters and duplexers are the corner stones in spectral management, having escaped miniaturization trends for a relatively long time; nowadays they are at the centre stage of these trends. As the telecommunication industry is experiencing its highest growth rates in the mobile sector, where the frequency bands allocated for these services are typically in the lower end of the microwave frequency ranges, miniaturisation is not a good to have feature, it becomes a pressing necessity. The difficulties encountered in miniaturising these components stems from some fundamental physical and technological limitations. These limitations are challenging researchers to push the limits of design techniques or fabrication technologies or both.

Our work subscribe to this general effort on the design technique front. The design technique chosen is that of topological optimisation to design miniature coupled resonator filters in Microstrip structures. It has the advantage that it can benefit from many of the fabrication technologies advancement in the future.

Organization

The thesis is organized as follows; in Chapter 1 we will present a system overview of the filters and duplexers in the context of multimode wireless systems. Then we introduce planar coupled resonators filters as a candidate approach for designing miniaturized RF filters. The system characteristics of these filters are explained followed by an introduction to the design parameters of these filters; those being, quality factor, coupling, and external quality factor. We conclude by a literature survey of the state of the art, followed by a brief comparison of the results reported by different design approaches in open literature.

Chapter 2 will serve as a theoretical introduction for the design of coupled resonator filters. We start with the introduction of **direct** coupled resonator filters and how to they synthesised from low pass prototypes, then a theoretical introduction of the transmission zeros, and how they are realised using coupled resonator.

In Chapter 3 we will present the technique employed to design miniaturized filters and duplexers. We start by presenting the $\lambda/4 \pm \delta$ wavelength resonator which is the basic resonator in our work. Subsequently, the resonator will be used to design two filtering structures, the symmetric feed and the non-symmetric feed. Using computer aided design and analysis we will compare the two structures to choose a candidate for miniaturisation. Once we have a candidate structure we will apply the topological optimisation technique to miniaturise the filter. Finally we will present the measurement of filters and duplexers fabricated via MHMIC process.

In Chapter 4 we will present the results of filters designed using the technique introduced in chapter 3 and lumped elements; both are designed targeting a high end MMIC process. The target process is called TQPED. This MMIC process of TriQuint Semiconductors is a process where typically several elements of the RF front (ex. LNA, PA) end can be integrated.

CHAPTER 1

RF FILTERS AND DUPLEXERS IN MODERN WIRELESS SYSTEMS

1.1 Introduction

Filters and Duplexers are integral components in virtually all wireless front ends. A typical architecture of a multimode front end is presented in figure 1.1. The architecture presented integrates Frequency Division Duplex -FDD (ex: WCDMA) system with Time Division Duplex-TDD (ex: GSM). In FDD systems transmission-reception (Tx-Rx) separation takes place in the frequency domain, this imposes constrains on the filtering elements utilised in the front-end and necessitates the use of a duplexer for frequency separation. While Tx-Rx separation in TDD takes place in the time domain, the RF front-end filters are still required to have strong attenuation characteristics. Another important distinction between TDD and FDD systems lies in the source of interference. While in TDD systems the major interferers lay outside the wireless device, in FDD systems interferers lay inside the module as leakage between the TX and RX paths in the front end.

In RF front-ends, diverse and often opposing requirements on different components tend to make the integration of all RF components using a single fabrication technology a challenge that proved resilient to definitive solutions. Consequently, manufacturers use different integration technologies to be able to meet required level of performance within the allowed area for each device simultaneously. The power amplifier for example is usually manufactured on a GaAs HBT (Gallium Arsenide Hetero Junction Bipolar Transistor) processes, a fabrication technology which provides good thermal characteristics that suits this component the best. The Mixer and LNA (Low Noise Amplifier) can be integrated into a single chip using a SiGe BiCMOS (Silicon-Germanium Bipolar Complementary Metal Oxide Transistor) process where low noise and good linearity can be achieved. Furthermore, a

significant effort has been put to integrate these modules in a system on package style providing excellent performance and miniaturization.

Unfortunately, antennas, filters and duplexers have largely eluded these miniaturization and integration trends. Filters and duplexers are high Q-factor passives of relatively large size - measured in terms of the guided wavelength- they are mostly external components to the other integrated circuits in the front-end.

Different solutions have been proposed for the design of miniaturized high-Q passives for RF fronts ends. The most popular of which is using acoustic wave technologies, these have found support from equipment manufacturers as acoustic wave filters quickly became the industry de-facto technology for miniaturized filters. Therefore, SAW (Surface Acoustic Wave) and BAW (Bulk Acoustic Wave) are found in every user terminal. A major disadvantage of these filters is that their fabrication process is incompatible with those of other components of the front end, also low power handling capacity; stability and a relatively high insertion loss are also concerns. Fabrication process incompatibility of acoustic wave devices stems from the characteristics of their fabrication processes; for SAW filters, fragility and the need of hermetic packaging inhibits their monolithic integration with active components [1]. On the other hand BAW filters have mechanical characteristics that are more integration friendly, but the materials used and the fabrication constraints required for BAW fabrication are largely different from the standard active devices fabrication process such that monolithic integration results in a more expensive, lower yielding process, therefore, monolithic integration of BAW integration is disadvantageous[1].

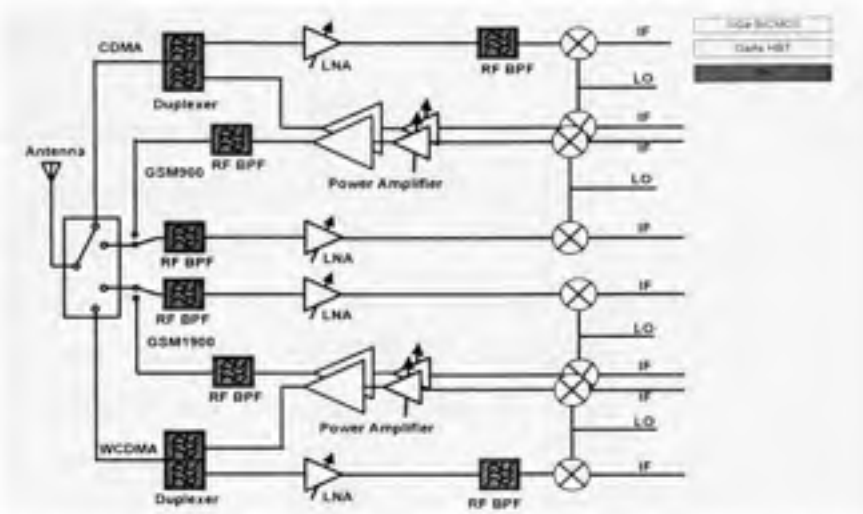

Figure 1.1 ***A multi-mode front end module with emphasis on integration technologies.***

Researchers have dedicated a lot of attention to planar filter and duplexer miniaturization in recent years owing to their ease of fabrication, seamless integration potential, power handling capability, stability and cheap price.

This renewed interest for technologies such as MHMIC and MMIC have produced significant advances in the design techniques of miniature planar filters. Planar fabrication processes have distinct advantages on other processes in terms of cost, integration, power handling and stability; moreover, these processes are mature and have proven to give high yield in a high volume context. The major disadvantage of these technologies is the inherent difficulty of designing filtering structures that accommodate low GHz frequency circuits having low insertion loss, small fractional bandwidth (<5%), and miniaturized size.

In this work we tackle the miniaturization problem of filters and duplexers targeting those fabrication technologies of active front-end components i.e. LNA and PA, these processes are fundamentally planar in nature of which MHMIC and MMIC processes are examples. Our technique is based on a topological optimization of folded half wavelength coupled resonators filter.

1.1.1 Planar RF Filters

Planar RF filters are these filters that use planar structures to realise the filtering elements. These filters are typically manufactured as MicroStrip (MS) or Coplanar Wave Guide (CPW) structures, whether distributed or lumped. Distributed planar filters tend to be relatively large due to the use of resonators whose sizes are comparable to the wavelength. At low GHz frequencies, the area occupied by these filters inhibits their use in many applications and eliminates the option of their monolithic integration in modern user terminal front-ends. While lumped component filters do not suffer from the aforementioned drawback; their power handling capacity and Q factor at high frequencies tend to be poor.

RF filters used in modern multi mode/band front ends are predominantly band pass filters with relatively low fractional bandwidth. To design such filters in planar structures; coupled resonators techniques are widely employed. Recently, cross coupling techniques are extensively utilised to insert finite frequency transmission zeros for enhanced skirt characteristics and reducing the number of resonators used in the filter; consequently reducing the filter size.

The system characteristics of filters that are of concern in the context of this current research are insertion loss, return loss, attenuation and relative size. These characteristics are defined as follows:

- **Insertion Loss (IL)**: Is the loss in signal power resulting from the insertion of the filter in the path of the signal. It is expressed as the ratio of the incident power P_{in} to its input port to the output power from its output port P_{out} in the pass band of the filter. This quantity is measured in terms of the transmission scattering network parameters (S_{21} and S_{12}) commonly used in vector network analyzers. These quantities are represented mathematically as:

$$IL=10\log(P_{in})-10\log(P_{out}) \qquad (1.1)$$

It is generally required that the insertion loss be kept to a minimum especially in the context of RF front-ends, where less than 3dB are typically accepted values.

- **Return Loss (RL)**: Is the power reflected from the filter as a result of impedance mismatch between the source and filter. It is expressed as the ratio of the incident power P_{in} to its input port to the reflected power from its input port P_{ref}. This quantity is measured in terms of the adaptation scattering network parameters (S11 and S22) commonly used in vector network analyzer. These quantities are represented mathematically as:

$$RL = 10\log(P_{in}) - 10\log(P_{ref}) \quad \textbf{(1.2)}$$

- **Attenuation**: The attenuation is a transmission characteristic of the filter; it can be considered the insertion loss in the stop band of the filter. It is measured by the same transmission scattering parameters as the insertion loss. In the context of multi band/mode operation it is imperative to distinguish two distinct frequency bands.

    - **Narrow Band Attenuation**: It is the attenuation characteristic of the filter near the pass band of the filter. This attenuation usually is specified as a required attenuation level at a finite frequency which in turn determines the required steepness of the filter and consequently the order of the filter.

    - **Wide Band Attenuation**: It is the attenuation characteristics of the filter up to and beyond the second harmonic of the central frequency of the filter. This characteristic is very important due to the inherent property of planar resonant structures to have repeated and spurious pass bands harmonics of the filter's central frequency. Special attention has to be given to assure that the wide band attenuation characteristic of the filter does not allow signals from other modes/bands to interfere with signals of the operational band.

Both of these characteristics are represented by the transmission scattering network parameters (S12 and S21).

- **Relative Size**: In the context of our research we will define the size of the filter as the minimum rectangle required to place the filter on a substrate. The rectangle's width and breadth will be measured in terms of the λ_g. Where λ_g is defined as the guided wavelength of a transmission line on the same substrate of the filter. For example a filter may occupy an area of 60mm×20mm while the guided wave length could be 11mm; then the filter size is $6\lambda_g \times 2\lambda_g$.

1.1.2 Duplexers

Duplexers are passive three port devices that allow a single antenna to be shared simultaneously by a transmitter and a receiver operating in close but separate frequency bands. The ports of a duplexer are transmission port, reception port, and an antenna port as depicted in Figure 1.2.

In the context of modern multimode FDD front ends, efficient utilization of the available bandwidth requires guard bands to be relatively small. Moreover, due to the large dynamic range between the transmitted signal and the received one – typically more than 70 dB – it is required that the duplexer provide steep separation between the two bands for proper functionality of the system and efficient bandwidth utilisation. It is worth noting that in FDD systems the noise is internally generated from the system; since there are two different RF signals propagating through the system.

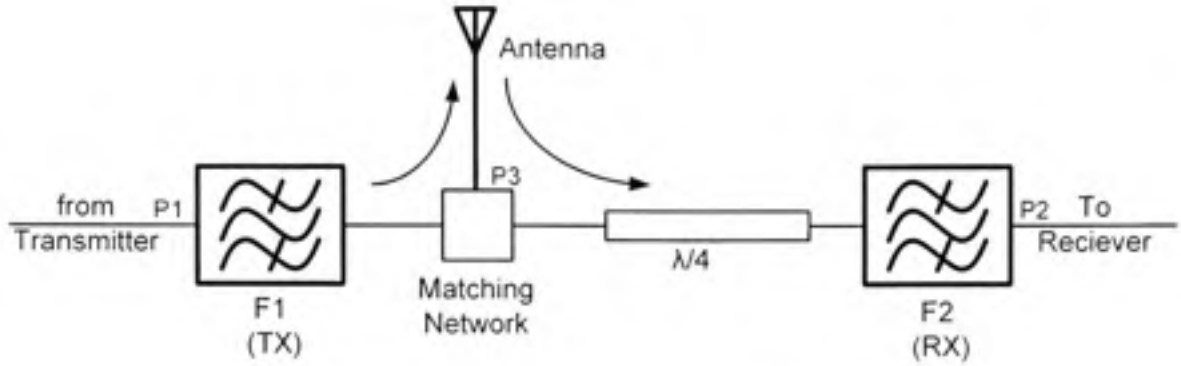

Figure 1.2 ***Duplexer architecture.***

Duplexers are made of two band-pass filters; one connects to the transmitter and the other to the receiver, each of these ports is a port of the duplexer. The other two ports - one of each filter - are separated by quarter wave transmission line and a matching network connecting the third output port of the duplexer to the antenna.

The system characteristics of duplexers of concern in the context of this current research are insertion loss, return loss and isolation and relative size. These characteristics are defined as follows:

- **Insertion Loss (IL)**: The insertion loss of the duplexer is defined similarly to that of the filter. The only difference is that duplexers have two distinct pass bands; one for the transmission, the other for the reception. The Insertion loss for the transmission band is commonly required to be about 1dB less than that of the receiving band.

- **Return Loss (RL)**: The return loss of the duplexer is defined similarly to that of the filter. The only difference is that duplexers have two distinct pass bands; one for the transmission, the other for the reception.

- **Relative Size**: Defined similarly to planar filters above.

- **Isolation**: It is the relative attenuation provided between the two paths of the duplexer; transmitter to antenna path and antenna to receiver path. As we indicated before this characteristic is of fundamental importance in the system because of the large dynamic between the transmitted signal and the received one.

    - **Tx in Rx band**: It is the attenuation provided by the duplexer for a signal having a frequency equivalent to that of the reception band when injected from the transmission port of the duplexer.

    - **Rx in Tx band**: It is the attenuation provided by the duplexer for a signal having a frequency equivalent to that of the transmission band when injected from the reception port of the duplexer.

1.2 Survey of pertinent research activities

Miniaturization efforts followed different approaches on both the fabrication and the design front. Since we are primarily concerned with the design aspects of miniaturization, we will present here the most pertinent approaches followed by different research teams in this field.

A direct approach for achieving highly miniaturized filters is to use lumped components; this achieves miniature filters but suffers very poor performance in terms of losses and steepness of attenuation when standard processes are employed. The origin of this poor performance is mainly that the quality factor of inductors and capacitors deteriorates rapidly at radio frequencies. Modern MMIC process can achieve high quality factor (>500) for capacitors, but quality factors for inductors remain very limited when using finite conductivity metals. In [2] High Temperature Superconductors (HTS) were used to realise a 3^{rd} order bandpass lumped elements filter, the use of HTS material allowed for the realisation of inductors with high quality factors. While results reported in [2] are satisfactory in performance and miniaturization, the filters use unique materials and fabrication process that are not directly

compatible with commercially available MMIC process; moreover, the use of HTS requires a cooling mechanism for materials to maintain their superconductive properties.

Another alternative to overcome inductor losses when designing lumped components filters is to use Q-enhanced or active inductors as suggested in [3]. This technique increases slightly the area of inductors used in the design but allows for arbitrary Q-factor. Problems of impedance matching between active and passive components, non linearity and stability tend to limit the application of these filters to IF frequency ranges. Furthermore, in the context of RF front ends, power efficiency is a major concern for battery operated user terminals; consequently the use of active components is not suitable.

A different approach for filter miniaturization has been developed around hair-pin filters. Hairpin filters are classical coupled resonator filters. The so called Hairpin structure is considered a folded form of half-wavelength transmission line resonators.

In [4] the arms of Hairpin resonator were folded for the purpose of filter miniaturization and direct coupling was used to produce a third order miniature filter. Further developments in [5] introduced structural improvement to the hairpin resonator and cross coupling techniques were introduced to provide a miniature and highly selective filter.

Finally, in [6] the filter introduced in [4] was realised using multilayer inter coupling on an LTCC (Low Temperature Co-fired Ceramic) process. This technique has produced excellent miniaturization results for a four quasi-elliptic band pass filter, but losses where relatively high for metal thicknesses accessible using this technology, also some divergence between the electromagnetic simulation and the measurements obtained due to the difficulties of simulating the multi layer inter coupling. Despite these problems this technique promises very high miniaturization potential and could prove to be very successful. It is worth noting that this technique can be utilized to further miniaturize the filters we developed, providing additional miniaturization for our filters.

Moreover, another approach is to use dual mode resonators. A dual mode resonator is a resonator that is designed to excite high order modes and recombine them at the output port. These modes have slightly different resonant frequencies which allows for the design of band pass filters. The miniaturization aspect stems from the fact that only a single resonator is required to design a filter. Good miniaturization can be achieved using this techniques but due to the sensitivity of the excited modes to the symmetry of the resonator, the size of the resonator remains larger than multi resonator filters designed by alternative techniques. An example of a miniaturized filter of this type is a fractal dual mode filter presented in [7].

Finally, another approach for filter miniaturization is to find a miniature topology with minimal Ohmic losses. In [8] a new methodology for topological compacting was introduced, also a set of filters and a duplexer for UMTS front end was designed and fabricated on a standard alumina substrate. The filters and the duplexer reported have achieved high performance and compact size. These are the most miniature filters to our knowledge in single layer Microstrip structures.

After we have reviewed the different approaches in designing planar filters, we will present a comparative table to compare the respective performance of each of these techniques.

Table 1.1

A comparative table between the different approaches

Approach	Fractional Bandwidth	Attenuation	Size	Central Frequency
Lumped Components (HTS)	0.844%	-60dB	10mmx3.5mm	1.7GHz
Hairpin multilayer	3.7%	-30dB	5x7mm 0.16X0.11	3GHz
Dual Mode Resonators (Fractal)	1%	-50dB	20mmx20mm 0.15X0.15	0.85GHz
Topological Optimization	2.5%	-45dB	9mmx7.5mm 0.125X0.15	2GHz

From the table above we can witness that the topological optimisation technique achieves high performance and excellent miniaturisation, for this reason it was chosen for further investigation in our work. It is our goal to reproduce the same performance reported in the above references, but none the less to improve on the miniaturization and simplicity of the topology used.

1.3 Conclusion

In this chapter we presented RF filters and duplexers in the context of modern RF front-ends. It is evident that with multimode/multi band requirements the number of RF filters is on the rise. This constitutes a fundamental thrust behind miniaturization and integration efforts. These efforts are considered an enabling element for the future of the personal telecommunication revolution. The reasons behind the interest for developing miniaturized planar filters were discussed and a review of the most mature approaches in this filed were presented. Finally a resume of the results reported in literature using the presented approaches establishes the viability of the topological optimization technique for further research. In chapter 2 we will present a theoretical back ground for the principal techniques for the design of planar coupled resonator filters.

CHAPTER 2

PRINCIPLES OF COUPLED RESONATORS FILTER DESIGN

2.1 Introduction

In this chapter we are concerned with building a knowledge base of the some of the most fundamental and widely used concepts in coupled resonators filter design. We start with the general theory of **direct** coupled resonator filters and their synthesis from low pass prototypes, then we will use general filter theory of lumped element techniques to illustrate the concept of transmission zeros at finite frequencies. Subsequently, we will explain how **in direct** coupled resonator topologies are used to realise transmission zeros at finite frequencies.

2.2 Design of direct coupled resonator band pass filters

Direct coupled resonator filters in their most elementary form could be represented as in Figure 2.1 below. All resonators are identical and are directly coupled to one another as depicted in the figure. The value of the coupling coefficient is denoted by $M_{n,n+1}$ and can be positive or negative. Coupling between non adjacent resonators is neglected. The coupling to the external ports is denoted by the external quality factor Q_e. Cohn in [9] has introduced a method for designing coupled resonators bandpass filters from lowpass prototypes. Later in [10] he applied his method to design a multitude of different strip line parallel transmission line resonators. The method is based on a theoretical derivation of an equivalent circuit for microwave coupled resonators such that the coupling between resonators acts as an ideal immittance inverter.

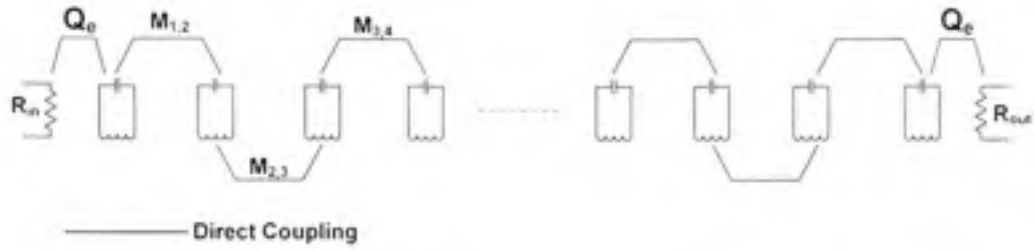

Figure 2.1 ***A general representation of direct coupled resonators filter.***

The goal of Cohn's method is to establish a relation between the circuit parameters of a prototype filter and the coupling parameters of the microwave resonators arrangement, i.e., the coupling coefficients $M_{n,n+1}$, and the external quality factor Q_e. Dishal in [11] has described an experimental method for finding the coupling coefficient and the external quality factor of coupled resonators. This method can be adapted to work in the context of modern electromagnetic simulation techniques instead of measurements. Therefore, using the combination of Cohn's formulation and Dishal's technique we can design bandpass filters from lowpass prototypes with relatively little effort.

It is important before further detail to mention that there are different quality factors that can be associated with circuit. Hence, it is important to discuss them and to identify the qualities they measure as well as the relation between them.

A quality factor is a ratio between energy storage and energy loss in a resonator. Depending on the origin of the losses being considered one can define three quality factors [12]:

$$\text{Unloaded Q:} \quad Q_u = \omega \frac{\text{Energy stored in theresonant circuit}}{\text{Power loss in the resonant circuit}} \tag{2.1}$$

$$\text{External Q:} \quad Q_E = \omega \frac{\text{Energy stored in the resonant circuit}}{\text{Power loss in the external circuit}} \tag{2.2}$$

Loaded Q: $$Q_L = \omega \frac{\text{Energy stored in the resonant ircuit}}{\text{Total power loss}} \quad \textbf{(2.3)}$$

These three factors are related by the following equation:

$$\frac{1}{Q_L} = \frac{1}{Q_E} + \frac{1}{Q_U} \quad \textbf{(2.4)}$$

In the planar filter design context we are more concerned with the external quality factor Q_e, as the unloaded quality factor Q_u has an upper limit that can not be surpassed for a particular fabrication technology. Also, it is very common that the values of Q_e required for realizing a filter is much lower than that of Q_u; and consequently becomes more dominant.

In this section we will explain in some detail how to derive the equivalent circuit as per Cohn's method. Then we will illustrate how Dishal's method was adopted to calculate the coupling coefficients using electromagnetic simulation.

2.2.1 Derivation of the equivalent circuit

Electric network circuit solutions are very well established and circuit capacitance and inductance values have closed form solutions for Chebychev and maximally flat type filters. The starting point is the lowpass filter prototype shown in Figure 2.2 where the circuit parameters $g_{1,2,3,\ldots,n}$ are the capacitances and inductances values as given by the tables for the n-even or n-odd filters. The value of r is generally taken to be unity except for the n-even for Chebychev responses. These values are available in virtually all references treating filter design of which [13] is an excellent example.

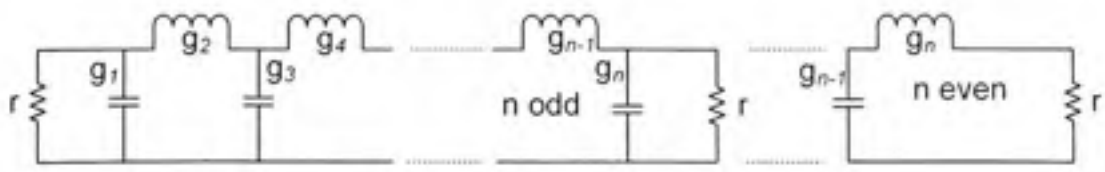

Figure 2.2 ***Low pass prototype filter of Chebychev or maximally flat response.***

To transform the lowpass prototype to a bandpass filter we use the lowpass to highpass transformation shown in Figure 2.3.

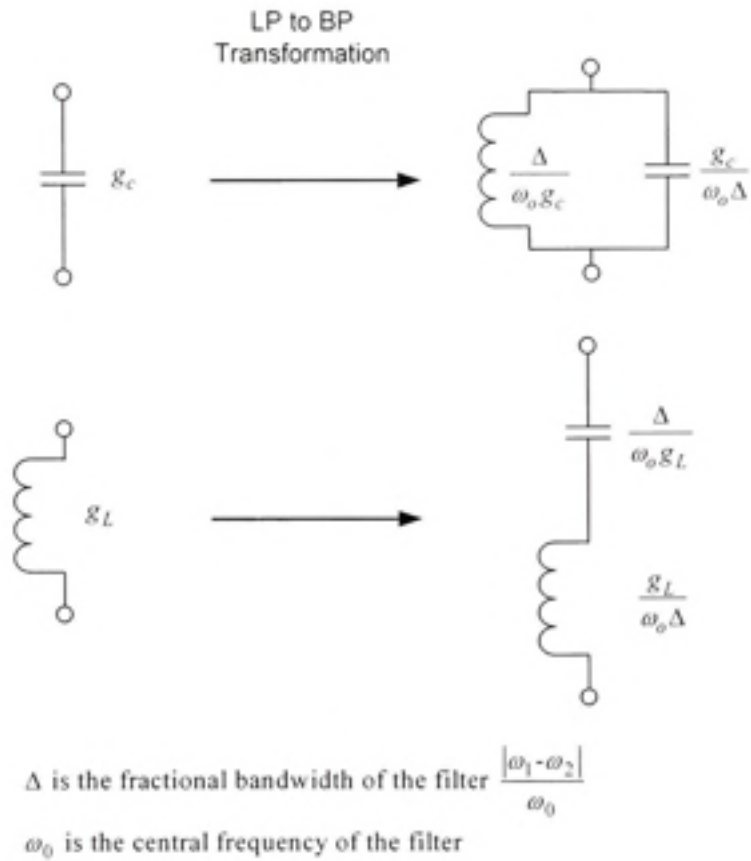

Figure 2.3 ***Lowpass to Highpass Filter Transformation.***

Applying this transformation to the lowpass prototype yields a bandpass filter with the corresponding bandwidth, central frequency, and attenuation characteristics as illustrated in Figure 2.4

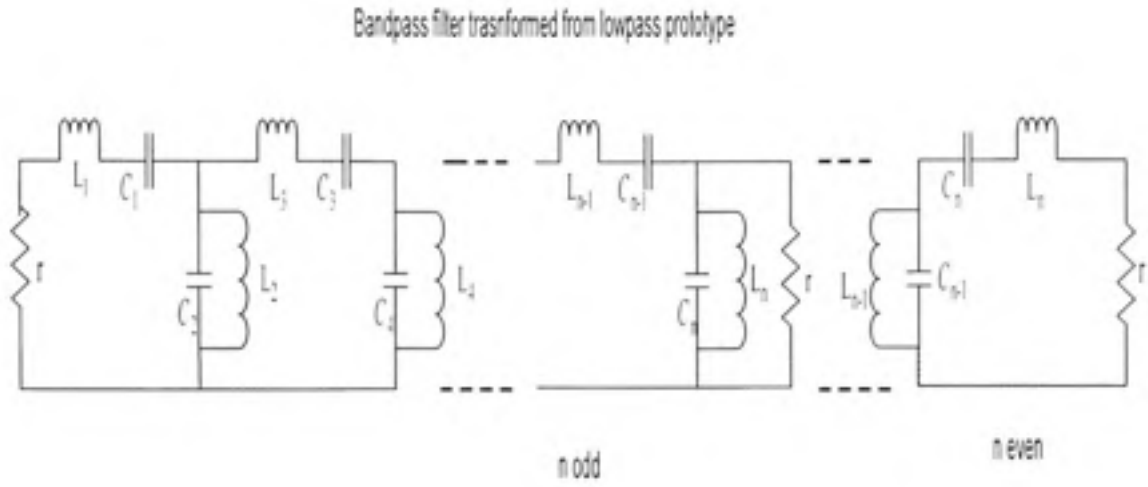

Figure 2.4 ***Trasnformed bandpass filter (Bottom) Circuit transformation.***

In order to transform the band pass filter to a form that approximates that of figure 2.1, we need to get rid of the parallel arms of the filter. Consequently, the next step is to transform the bandpass filter to an equivalent circuit with only series or parallel resonator sections and immittance transformers. Immittance transformers allow the transformation of a series section to a parallel section and vice versa [7].

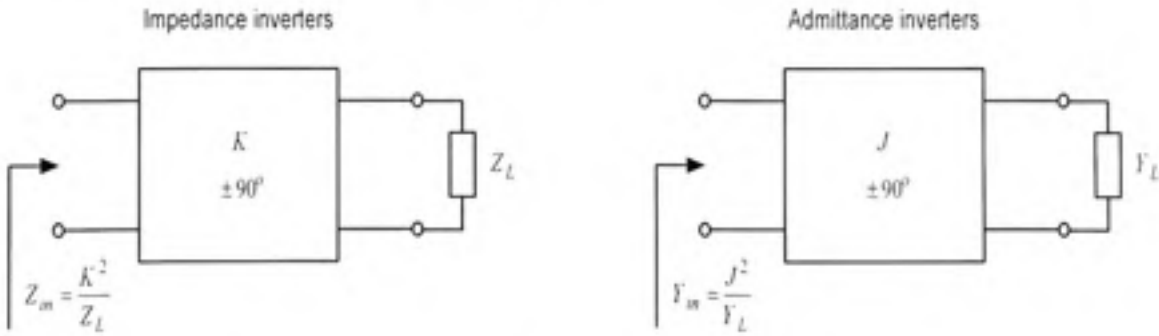

Figure 2.5 ***Conceptual operation of immittance inverters.***

The conceptual operation of immittance transformers, also called inverters, is illustrated in Figure 2.5. It was demonstrated by Dishal in [11] that these immittance transformers can be

realized using electromagnetic coupling. Using these circuit transformation and electromagnetic coupling as immittance transformers we obtain the required form of the filter depicted in figure 2.1.

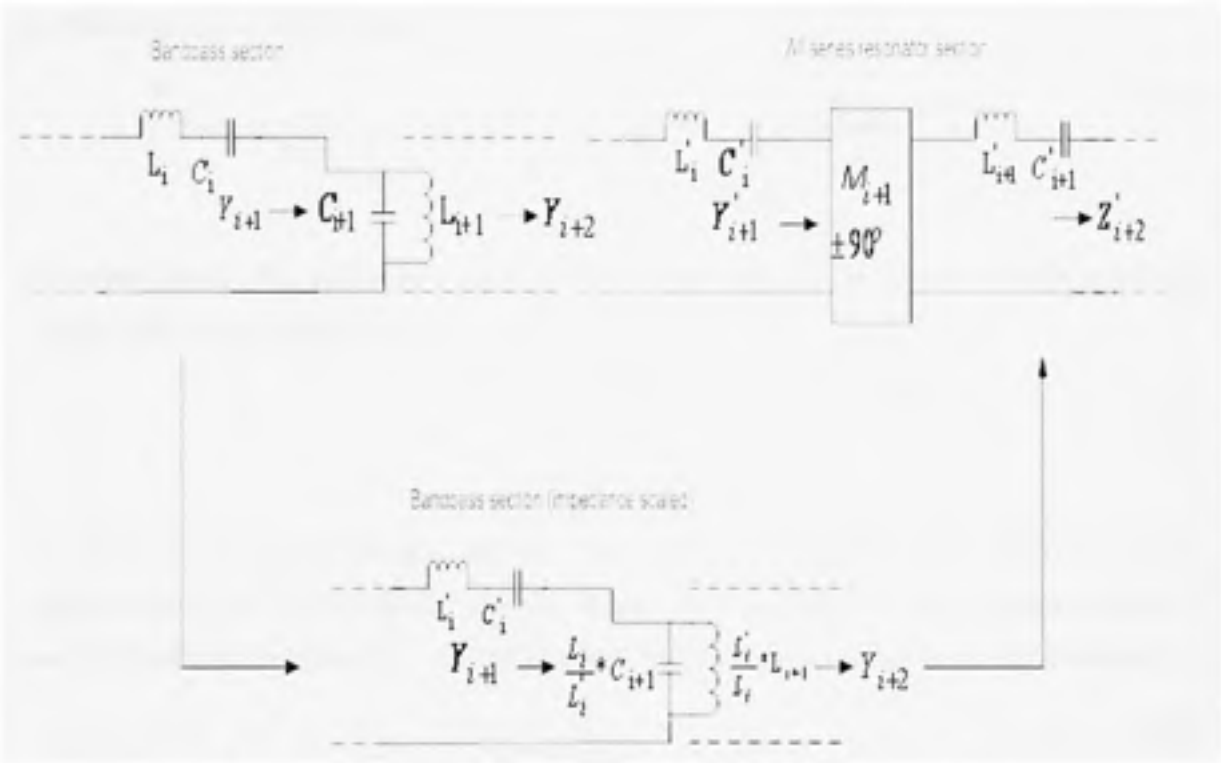

Figure 2.6 ***Step-by-step band pass section transformation***

Figure 2.5 illustrates the step by step band pass section transformation, where L_i,C_i are the inductance and capacitance of the $i^{th.}$ Section of the filter, Y_{i+1} is the input admittance of the i^{th}+1 section of the filter after impedance scaling. Finally $Y`_i$ and $Z`_i$ are the input admittance and impedance respectively of the final transformed section.

The first step in the transformation is to scale the impedance of the $i^{th.}$ bandpass section to have the same series resonance arm as the all series resonator sections as illustrated in Figure 2.6. This requires that all the other filter coefficients be also impedance scaled. It is to be

noted that $L_i^{'}$, $C_i^{'}$ are the values after transformation and L_i, C_i are the original bandpass filter values. For these sections to be equivalent the following condition must be satisfied:

$$Y_{i+1} = Y_{i+1}^{'} \tag{2.5}$$

Expanding this condition yields:

$$j\left(\omega C_{i+1} - \frac{1}{\omega L_{i+1}}\right)\frac{L_i}{L_i^{'}} + Y_{i+2} = \frac{1}{K_{i,i+1}^{2}}\left\{j\left(\omega L_{i+1}^{'} - \frac{1}{\omega C_{i+1}^{'}}\right) + Z_{i+2}^{'}\right\} \tag{2.6}$$

After identifying the quantities that have the same dependence on ω [9] and using the transformation identities in Figure 2.3 we find:

$$K_{i,i+1} = \frac{\Delta}{f_0}\sqrt{\frac{L_i^{'}L_{i+1}^{'}}{g_i g_{i+1}}} \tag{2.7}$$

The same procedure for the first and last sections of the coupled resonator filter yields the expression for the external quality factors. Moreover, it is a general practice that resonators used in the design are identical. Consequently the following forms are generally preferred:

$$Q_e = \frac{f_0}{\Delta} g_1 \tag{2.8}$$

$$M_{i,i+1} = \frac{\Delta}{f_0}\sqrt{\frac{1}{g_i g_{i+1}}} \tag{2.9}$$

These formulas relate the normalised coupling coefficient to a lowpass prototype such that the ripple and the attenuation response of the filter are preserved. It is to be noted that this method achieves good results only for low to moderate fractional bandwidth bandpass filter because it completely neglects the dependence of the coupling coefficient on frequency. The utility of these equations is not directly related to any particular resonator, consequently any arbitrary resonator can be used to realise the filter. To realise the required filter it is

necessary to be able to achieve the coupling coefficients values required by the equations above. The coupling is mainly dependant on geometrical parameters and is determined by either experiment and/or electromagnetic simulation as explained in the following section.

2.2.2 Extraction of coupling coefficients using electromagnetic simulation

The coupling coefficients between resonators $M_{i,i+1}$, the external quality factor Q_e, and the unloaded quality factor Q_u are the only parameters a designer is required to know in order to realise a bandpass coupled resonator filter as we have previously illustrated. Once the basic resonator is chosen, the unloaded quality factor Q_u is fixed and is mainly controlled by the fabrication technology parameters such as; metal conductivity, substrate loss tangent, and metal thickness. Consequently, the design parameters of interest are Q_e and the coupling coefficients $M_{i,i+1}$. In [11] a detailed method, referred to as Dishal's procedure, for measuring these parameters is presented. In this section we are concerned with the application of this method using ADS/Momentum electromagnetic simulation [14].

The setup for measuring the coupling coefficients between two half-wavelength Microstrip resonators is shown in Figure 2.7. The method calls for detecting the amplitude response to an excitation from a source that lightly loads the resonator (i.e. decrease the unloaded quality factor by less than 10%). From the amplitude response the coupling coefficient and the external quality factor are calculated by recording the peaks, the frequency difference between these peaks, and the fractional bandwidth of the response. Consequently, for different values of the geometrical parameters X and δ one can calculate both coefficients for any desired configuration. We will carry out this procedure via ADS\Momentum using a co-simulation technique. The co-simulation technique permits the simulation of circuit elements, lumped or distributed, and distributed layout components simultaneously. The layout components are simulated via electromagnetic simulation and the circuits are

simulated based on their respective circuit models. Using this technique a parameterized layout of the coupled resonators was built and very low lumped capacitors were used to lightly couple the ports of the resonators.

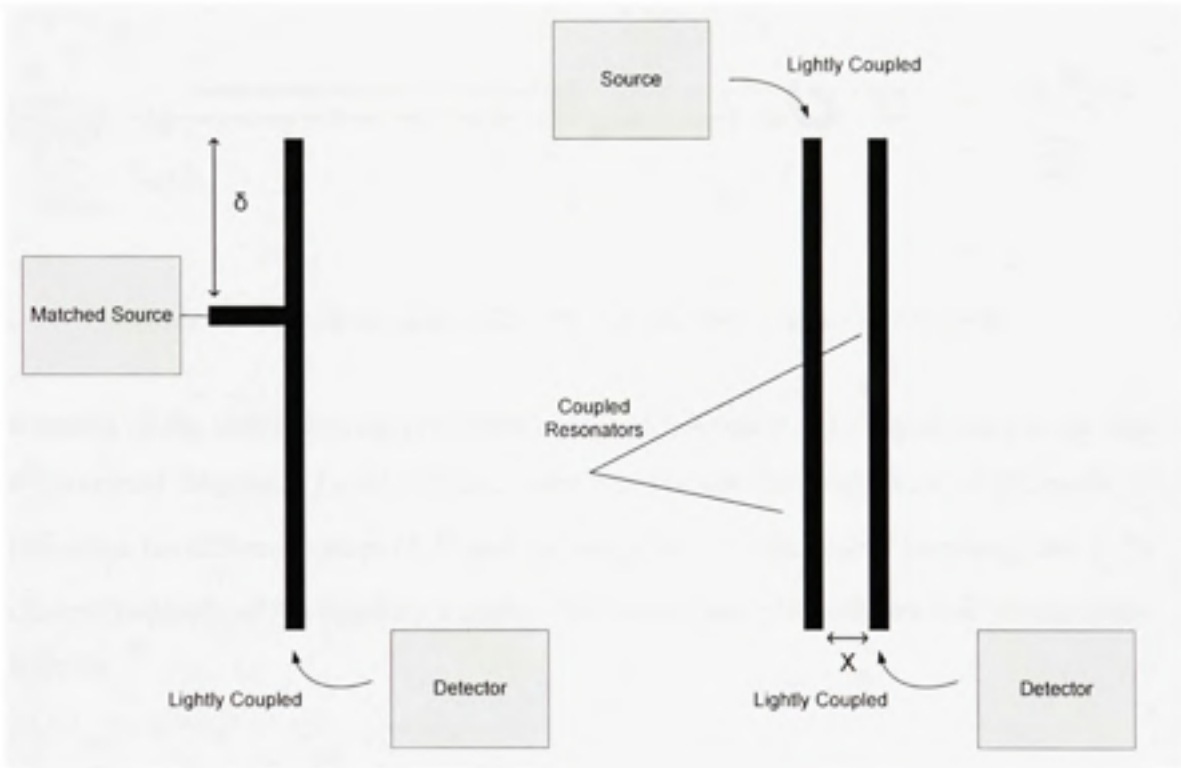

Figure 2.7 ***(Left) Setup for Q_e measurement (Rigth) Setup for K measurement.***

2.2.2.1 Extracting of coupling factor M

The circuit in Figure 2.8 is used to calculate the coupling coefficient M between the resonators for different values of the distance X between them.

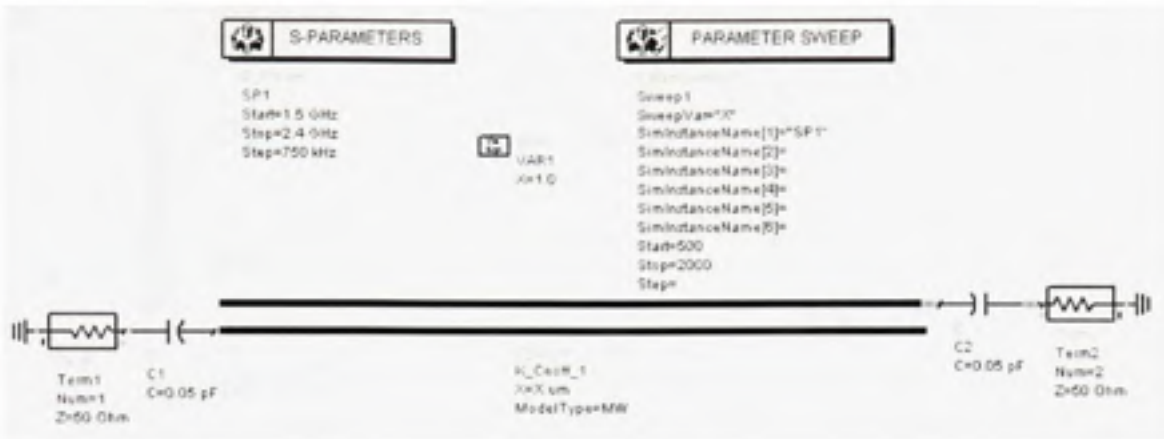

Figure 2.8 ***Circuit co-simulation for determining coupling coefficient.***

The results of the simulation are presented in Figure 2.9 below. By inspection we can find that the central frequency f_0 is 1.85GHz. Also we can note the frequencies of the peaks on the response for different values of X and we designate f_h to the higher frequency and f_l to the lower frequency of the response's peaks. The coupling coefficient can then be calculated as follows:

$$M = \frac{f_h - f_l}{f_0} \tag{2.10}$$

The following table summarises the results for the different values of X.

Table 2.1

The values of the coupling coefficient M

Separation X (μm)	500	1000	1500
Coupling Coefficient M	0.0784	0.0346	0.0162

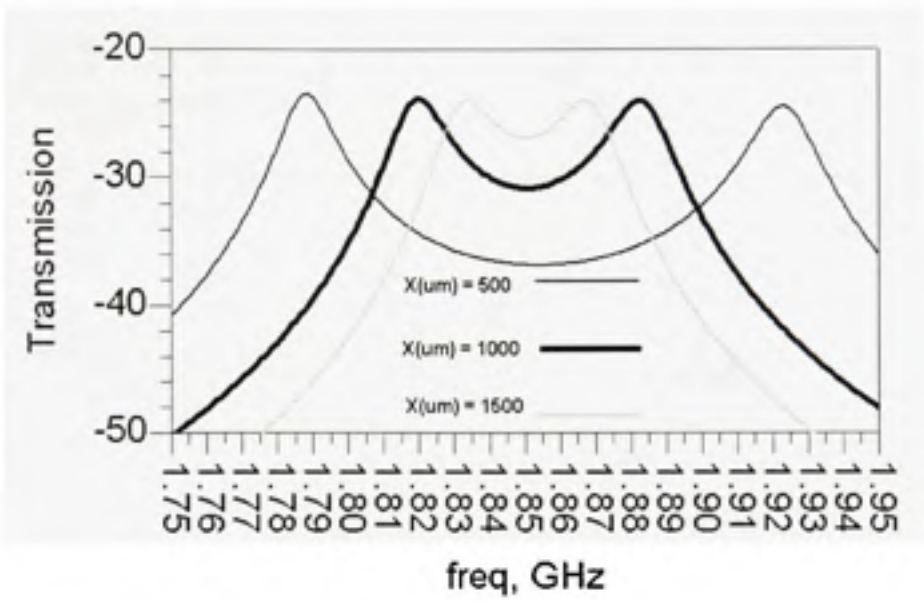

Figure 2.9 ***Extracting of the coupling coefficient between two resonators.***

2.2.2.2 Extracting of external quality factor Q_e

The circuit presented in Figure 2.10 below is used for the determination of the external quality factor, whereby we note the peak and the 3dB frequencies on the transmission curve of Figure 2.11. We then apply the following equation to find the required values.

$$Q_e = \frac{f_0}{\Delta} \tag{2.11}$$

The results of applying the above equation are presented in the Table 2.2.

Table 2.2

The values of the coupling coefficient Q_e

δ (μm)	16000	16500	17000
Q_e	124	78	47

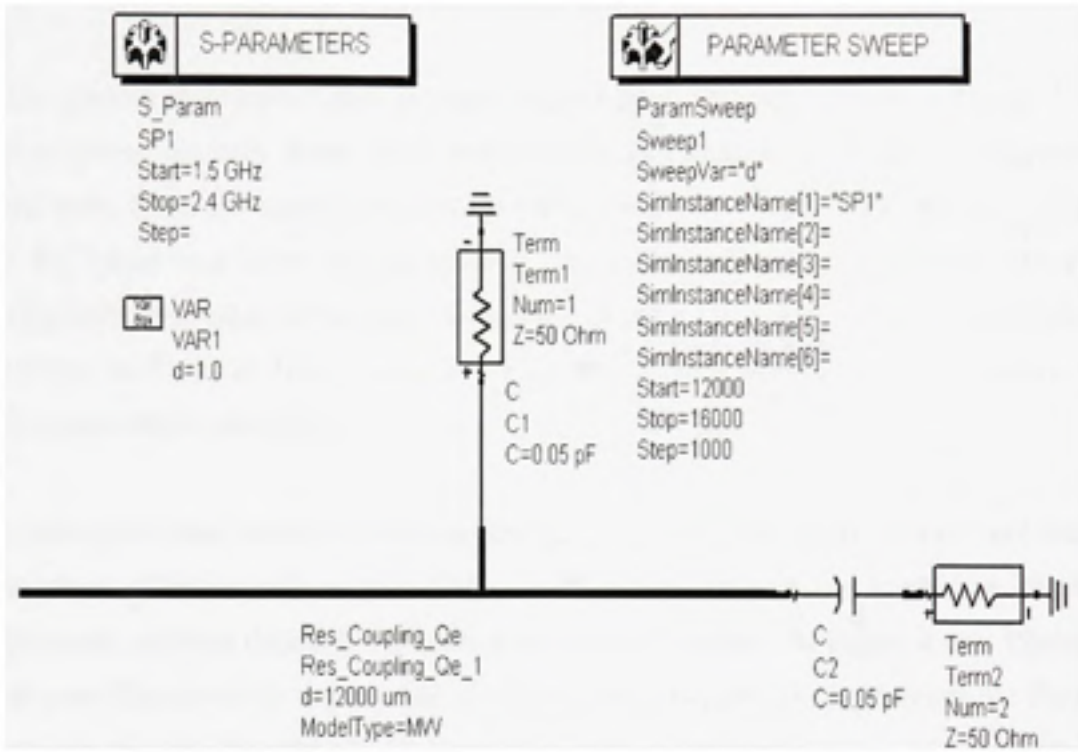

Figure 2.10 ***Circuit Co-simulation for determining external quality factor.***

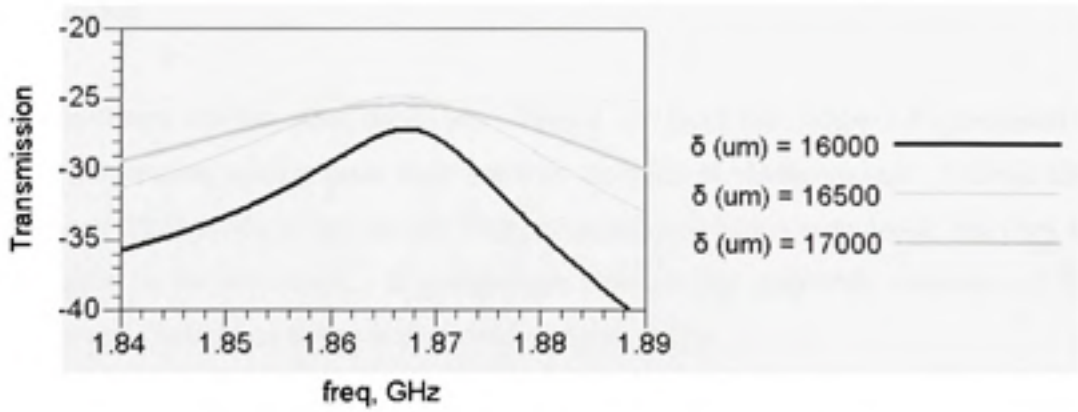

Figure 2.11 ***Determination of external quality factor.***

2.2.3 Transmission zeros at finite frequencies

Direct coupled resonators filters are very versatile and relatively simple to design. Despite their attractive features, these filters can only realise Chebychev pass band characteristics. When these filters are used at relatively low frequencies and high selectivity is required, the size and losses tend to be very prohibitive. A way to realise highly selective filters is to design filters that achieve transmission zeros at finite frequencies. These filters have high selectivity with lower filter order, and constitute a very interesting alternative for high performance band pass filters.

A transmission zero occurs is when no transfer of power between the source and the load takes place. Chebychev band pass filters, whether they are based on lumped or distributed components, achieve their zeros at infinite and zero frequency. In Figure 2.12 a Chebychev band pass filter circuit is represented at infinite frequency and at zero frequency. From the figure we can note that the C2, L1, and L3 provide a transmission zero at zero frequency, while C1, L2, and L4 provide a transmission zero at infinite frequency. Also, we note that a 3rd order Chebychev filter will provide an equal number of zeros at zero and infinite frequencies.

Elliptic filters, on the other hand, are a family of filters that achieve transmission zero at finite frequencies, giving them their superior attenuation characteristics. Elliptic filters are similar to Chebychev filters in that they are equiripple in the pass band, but they are also equiripple in the stop band. A comparison between the amplitude response of 3rd order elliptic and Chebychev filters is presented in figure 2.13.

Elliptic filters have better attenuation characteristics because of the existence of finite frequency transmission zeros in their response. Unfortunately, transmission zeros come with the price of non linear phase response which is quite important in the context of telecommunication terminals. Phase equalisation can be achieved using phase equalisation

sections at the cost of larger filters. Alternatively, quasi-elliptic filters can approach linear phase by placing transmission zeros at imaginary frequencies [15]. In the next section we will present how to practically linearize the phase response of coupled resonator filters using this approach.

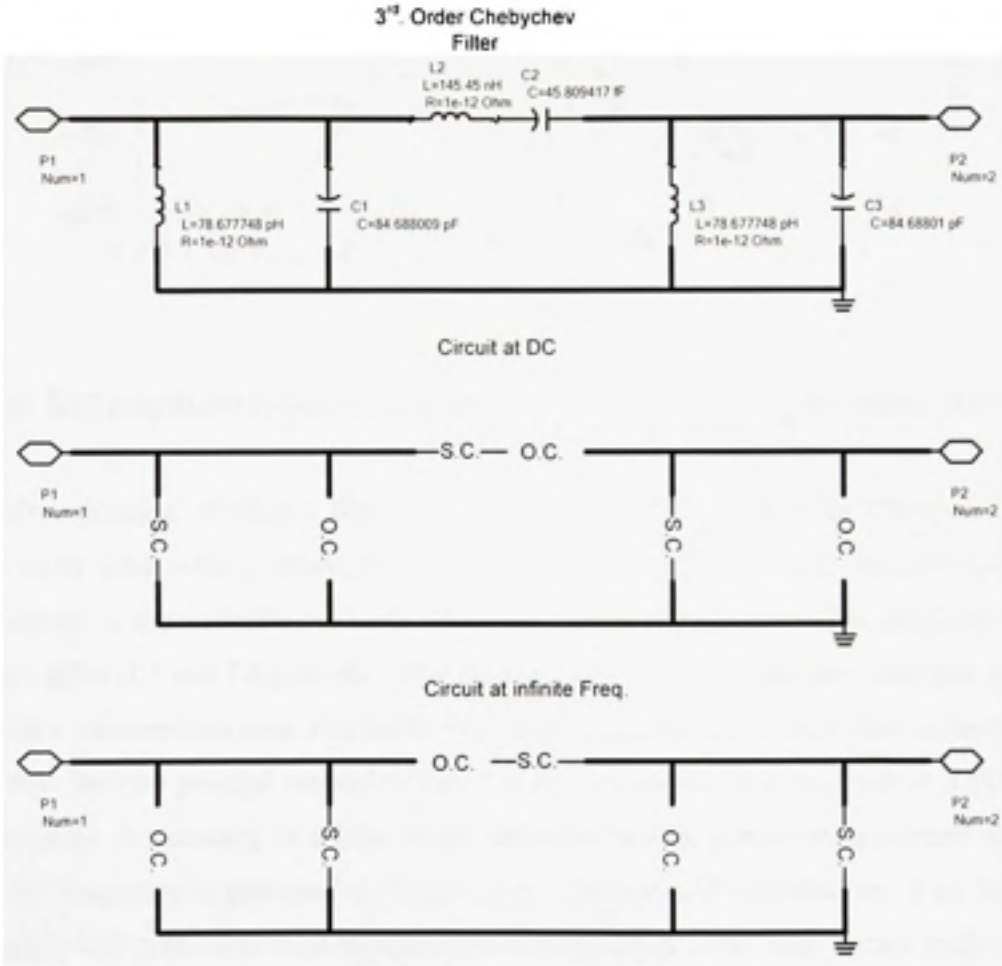

Figure 2.12 ***3rd. Order Chebychev filter at different frequencies.***

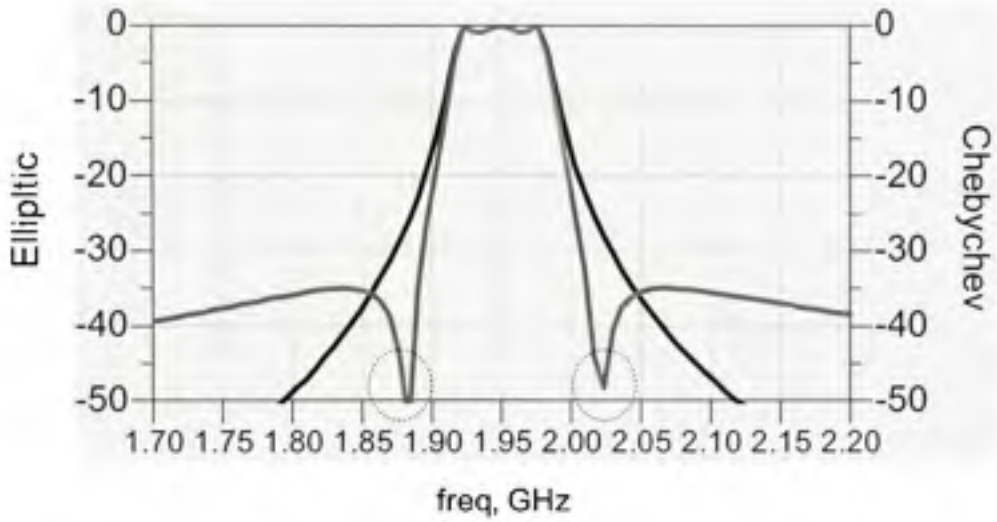

Figure 2.13 ***Amplitude response comparison between Chebychev and elliptic filters.***

The circuit realisations of elliptic filters are more complex than those of the Chebychev. For the third order filter whose amplitude response is shown in figure 2.13, the corresponding circuit diagram is shown in figure 2.14. We can see from these figures that, similarly to the Chebychev filter, L1 and L4 provide a transmission zero at zero frequency, and that C1 and C4 provide a transmission zero at infinite frequency. But unlike its Chebychev counter part, we find that the two parallel resonators provide two transmission zeros each at a different finite frequency. A summary of all the circuit elements providing transmission zeros at finite and infinite frequency is provided in Figure 2.15. The parallel combination of an inductor and capacitor will provide a transmission zero corresponding to an open circuit in the signal path when inserted in series with respect to the other resonators. By analogy, the series combination of an inductor and a capacitor will provide a transmission zero corresponding to a short circuit in the signal path when inserted in parallel to the other resonators.

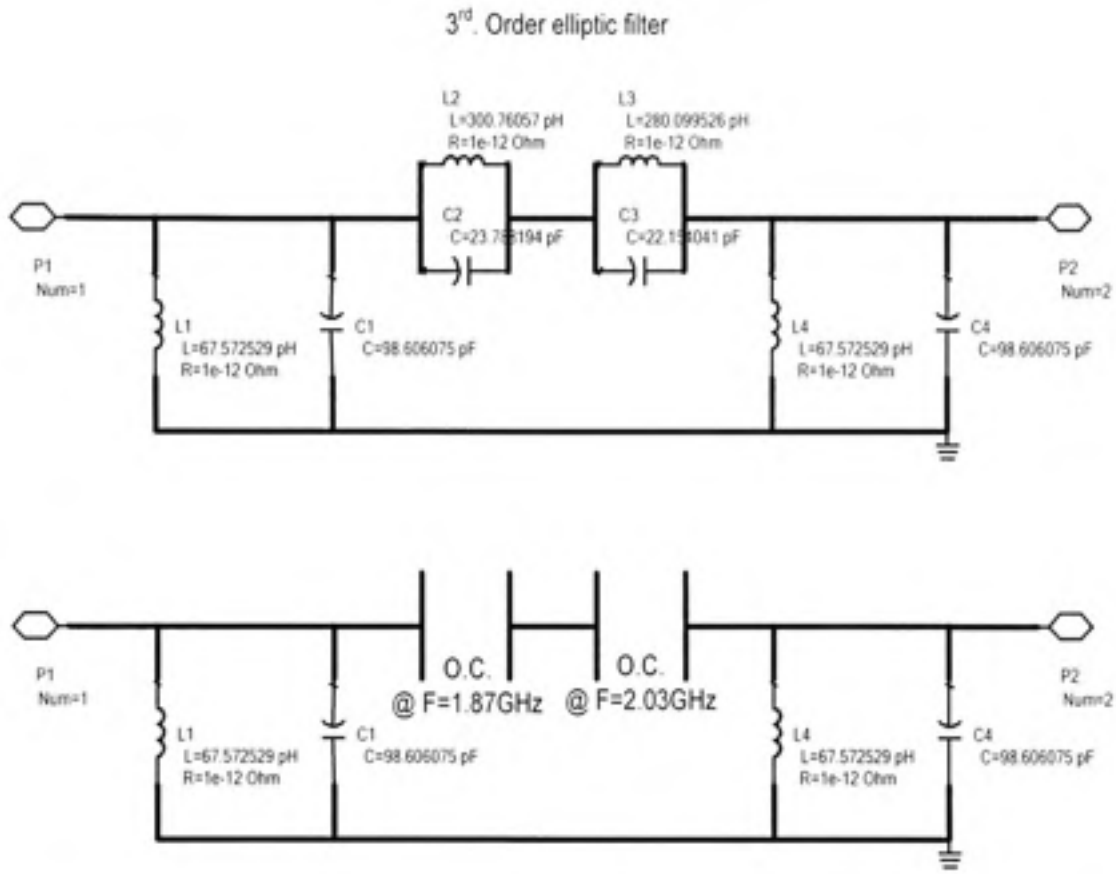

Figure 2.14 ***Circuit diagram for 3rd order elliptic filter.***

As we have seen in this section, transmission zeros have a profound effect on the attenuation characteristics of a filters when they are achieved at finite frequencies. Filters that have finite frequency transmission zeros can have very steep attenuation with relatively low order, making them a very attractive alternative when miniaturised filters are required. Coupled resonators filters can achieve finite frequency transmission zeros, if non adjacent resonators are allowed to be electromagnetically coupled. A more detailed study is presented in the next section.

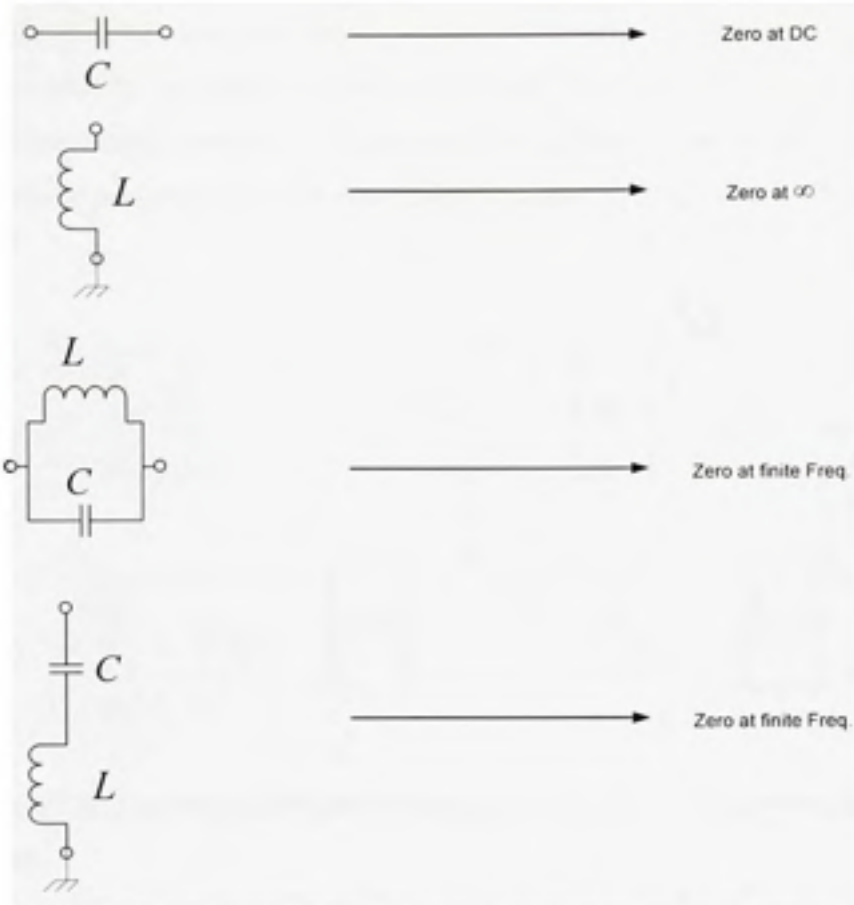

Figure 2.15 ***Circuit elements providing transmission zeros.***

2.2.4 Coupled resonator filters with a single pair of transmission zeros

Elliptic and quasi-elliptic coupled resonator filters can be achieved using cross coupling; which is the coupling between non adjacent resonators. Usually a bandpass filter can benefit from a pair of transmission zeros with only a small increase in circuit complexity. Resonant structures and the general coupling between them to achieve transmission zeros at real or imaginary frequencies is a very active area for research. Several canonical structures like the cascaded quadruplet and the cascaded trisections have been studied and realised as reported in open literature [4-6, 15].

In [15] an approximate synthesis method has been introduced for such filters. The basic principal of theses filters is to start from a low pass Chebychev prototype filter and introduce an admittance inverter such that a zero can be inserted in the filter response. The effect of inserting this admittance inverter is to mismatch the filter in the pass band. To re-establish a good match in the pass band, the values of the other admittance inverters have to be adjusted.

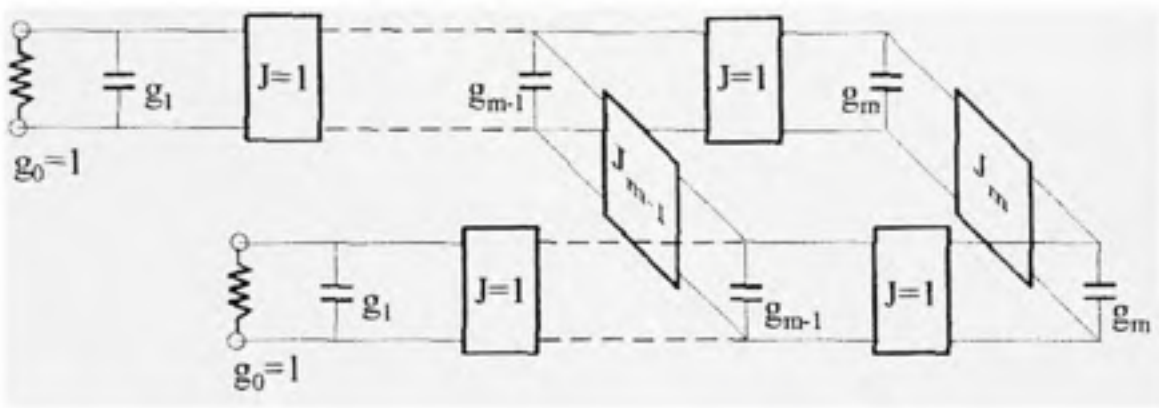

Figure 2.16 ***Low pass Chebychev prototype with poles at finite frequency [7].***

The filter prototype presented in Figure 2.16 achieves the pair of poles due to the insertion of the inverter denoted by J_{m-1}. In order to introduce the zero at a frequency f_a the required value of J_{m-1} is given by

$$J_{m-1} = \frac{-J_m^{'}}{(\omega_a g_m)^2 - J_m^{'2}} \tag{2.12}$$

Where $J_m^{'}$ is a slightly changed value of J_m as in (2.9)

$$J_m^{'} = \frac{-J_m}{1 + J_m J_{m-1}} \tag{2.13}$$

It is to be noted that in [15] equations for imaginary frequency transmission zero insertion were introduced. A filter based on square open loop resonators is presented in figure 2.17 as an example for filters with a pair of transmission zeros at finite frequencies and its response is shown in figure 2.18. The bottom resonators of the 8th order filter are responsible for the transmissions zeros (encircled in the figure 2.18) as they are cross coupled to the principal resonators arrangement.

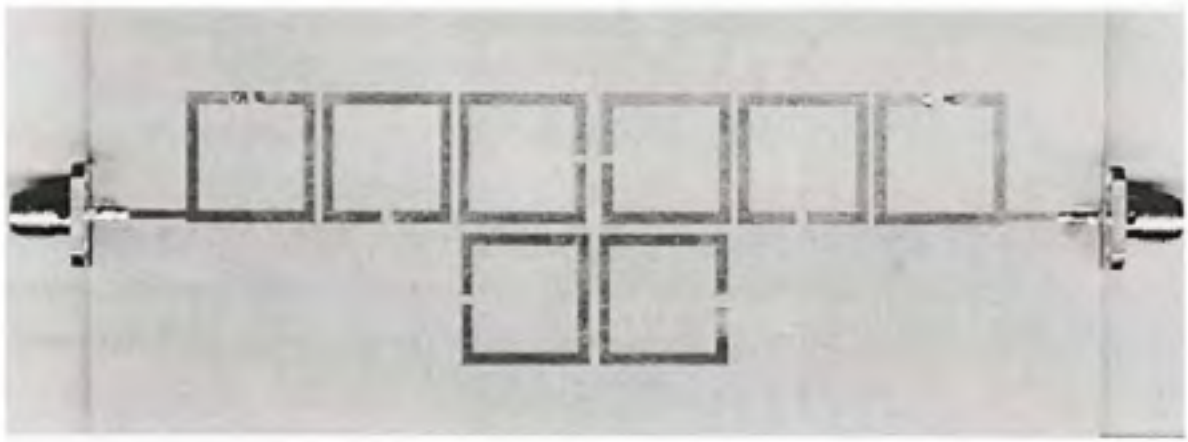

Figure 2.17 ***Square loop coupled resonator filter with resonators cross coupling from[7].***

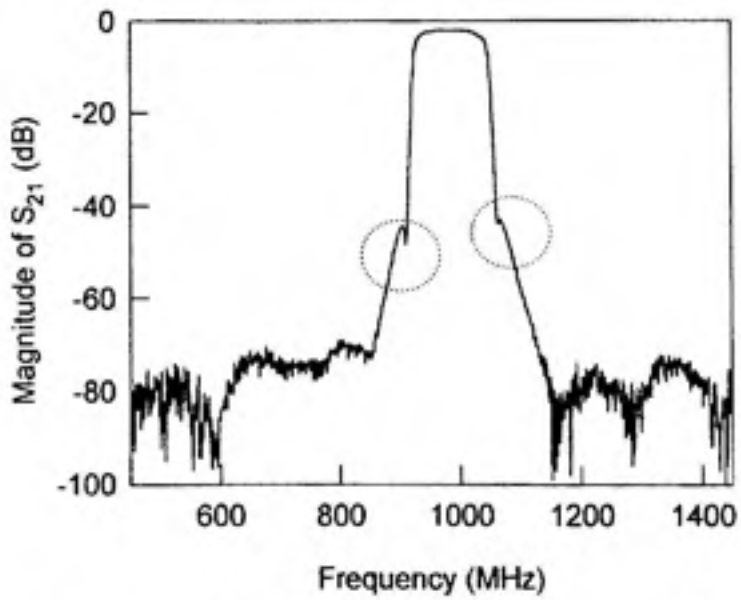

Figure 2.18 Transmission response for filter in figure 2.17 above [7].

The coupling arrangement presented in figure 2.17 is used to introduce transmission zeros at finite real frequencies. This has the effect of enhancing the attenuation of the filter. Alternatively, if it were required to linearize the phase response of the filter, it would have been possible to do so by inserting these zeros at finite imaginary frequencies. A straight forward technique to achieve this is by changing the type of coupling of the cross coupled resonators. More precisely, the general coupling scheme in figure 2.17 is inductive coupling and if capacitive coupling were used to couple the bottom resonators, then transmission zeros would to be inserted at imaginary frequencies and a linearized phase response is achieved.

2.3 Conclusion

In this chapter we have presented some of the most common techniques for designing coupled resonator filters. We have also detailed one of the more advanced techniques in filter design, i.e. introduction of transmission zeros at finite frequencies. The insertion of transmission zeros constitutes a fundamental technique on which our work is based. However, it is to be noted that in our work we use geometrical optimization for filter miniaturisation. If we were to use the cross coupling technique as in traditional method, it would have been necessary to re-extract the coupling coefficients and external quality factor for the resonators each time the geometry is changed.

CHAPTER 3

FILTERS AND DUPLEXERS IN MHMIC TECHNOLOGY

3.1 Introduction

In this chapter we present the design methodology adopted in this work in greater detail and its application to realise filters on MHMIC substrates. First we introduce the $\lambda/4 \pm \delta$ resonator which is the basic resonator in our work. Subsequently, we use the resonator to design a second order filter. Two filter structures will be presented: the symmetrical feed and the asymmetrical feed structures. Each of these structures exhibits different transmission zero location. After evaluating the two structures, a candidate structure will be selected for miniaturisation. Filter miniaturisation is achieved via a geometrical optimization technique which will be thoroughly studied. Finally, we will present the measurements of filters fabricated on MHMIC substrates.

To illustrate our design technique we will use both circuit and electromagnetic simulations to study the response of different filter structures. We begin with a single resonator, followed by a simple two resonator filter, and finally we present the miniaturization technique and its application to the filter structure. In each step we will study the effect of relevant geometrical design parameters such as the spacing between resonators and the displacement of the feed point. In general terms, the optimality criteria for the geometrical optimisation technique used will be the size of the filter and its performance. In other words, the minimum filter size that fulfills the performance requirements will be considered optimum.

The Advanced Design System[1] of Agilent Technologies will be used to perform the studies mentioned above. Also, we have chosen to perform these simulations on a single substrate configuration and in the frequency band of 1.8-2.3 GHz, which covers both the PCS and UMTS bands. The layers arrangement of the used substrate is presented in Table 3.1. When another substrate is utilized it will be explicitly indicated.

Table 3.1

Layers arrangement of the default substrate in this work

Layer	Material	Function	Thickness (μm)	Relative Electric Permittivity	Electric Conductivity (S/m)	Loss tangent
0	Copper	Ground	-	-	5.8e7	-
1	Alumina	Substrate	254	9.98	-	0.0001
2	Gold	Metallization	6	NA	4.1e7	-

The fundamental characteristics of a Microstrip line on the above substrate are presented in Table 3.2 below.

Table 3.2

Geometrical and electrical characteristics of used transmission line

Electrical		Geometrical	
Characteristic impedance Z_0 (Ω)	50	(W)idth μm	254
Electrical length (Deg.)	90^o	(L)ength μm	15000

[1] Advanced Design System: A suite for RF System and circuit simulation provided by Agilent technologies.

3.2 The λ/4±δ Resonator

This resonator was first introduced in [16] and can be viewed as the generalisation of the $\lambda/2$ resonator. The basic structure of the resonator is depicted in the Figure 3.1 below. The structure is formed by two parallel open circuited transmission line stubs of the same electrical length save a small distance δ where $\delta << \lambda$. Although, this representation neglects the width of the feed point as well as the effect of branching to the load impedance R_0, it is nonetheless representative of the physics of the structure. Using these simplifications we obtain the mathematical expression for the unloaded quality factor Q_u [12] as follows:

$$Q_u \approx \frac{\pi}{2\alpha(l_- + l_+)} \tag{3.1}$$

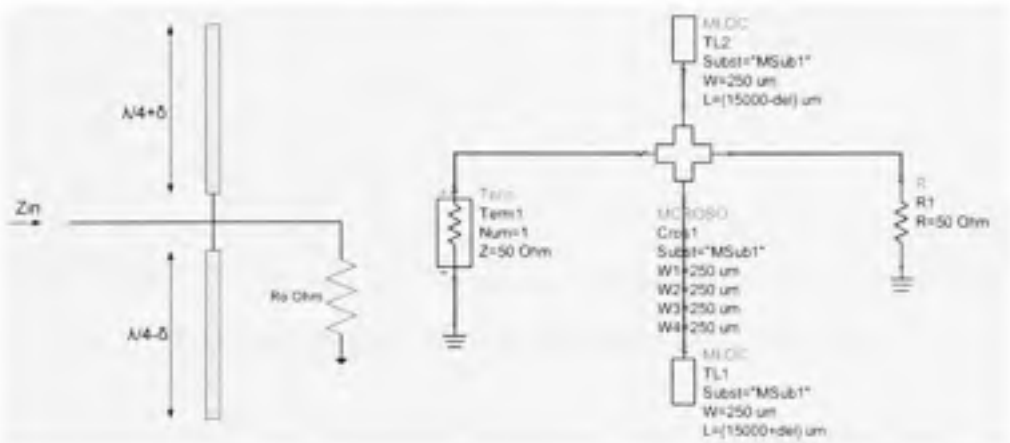

(a) (b)

Figure 3.1 ***Structure of the λ/4 ± δ resonator: theoretical model (a), circuit model (b).***

Where α is the attenuation constant of the stubs in nepers per meter and l- and l+ are the .... such that $l_- + l_+ = \lambda/2$. Both parameters α and $\lambda/2$ can be calculated by using the LineCalc utility in ADS for different substrate configurations as shown in Figure 3.2. For this type of resonator, equation 3.1 yields unloaded quality factors on the order of 100 to 400

for typical commercially available substrates of different metallization thicknesses and dielectric constants.

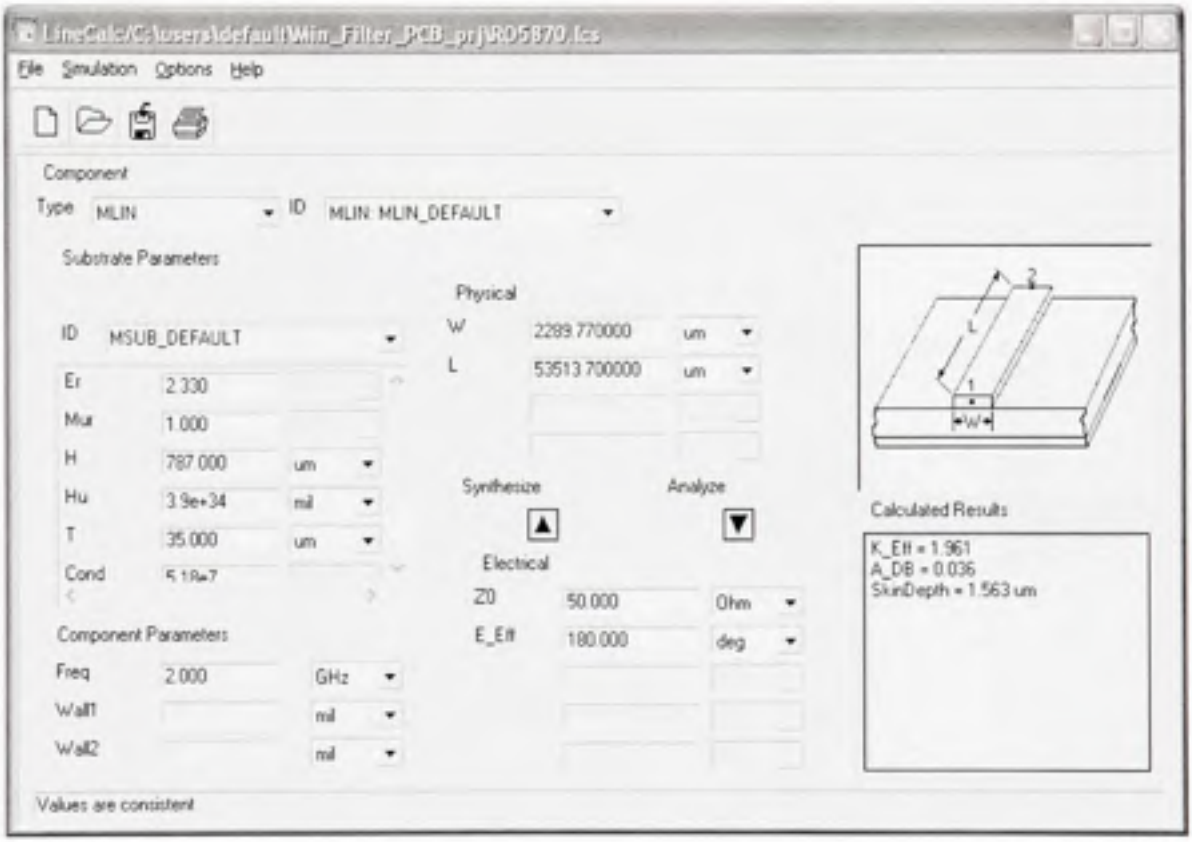

Figure 3.2 ***LineCalc showing resonator loss as A_DB.***

On the other hand, the loaded quality factor Q_l of this resonator has different characteristics. To calculate the loaded quality factor of this resonator we will use the results of circuit simulation of the circuit of Figure 3.1. The loaded quality factor can be calculated from the magnitude of the input impedance Z_{in} curve using the following formula:

$$Q_l = \frac{f_o}{\Delta f_{3db}} \tag{3.2}$$

Where f_o is the resonance frequency (where Z_{in} attains its maximum value for the configuration used above) and Δf_{3db} is the bandwidth where $|Z_{in}| \leq |Z_{in}|_{\max} / \sqrt{2}$ on the Z_{in} curve. Figure 3.3 illustrates the variation of $|Z_{in}|$ or mag(Zin) with the frequency for several values for the feed point displacement "δ". In Figure 3.4 the loaded quality factor Q_L is presented as a function of the feed point displacement, values for Q_L are calculated from the values presented in Figure 3.3.

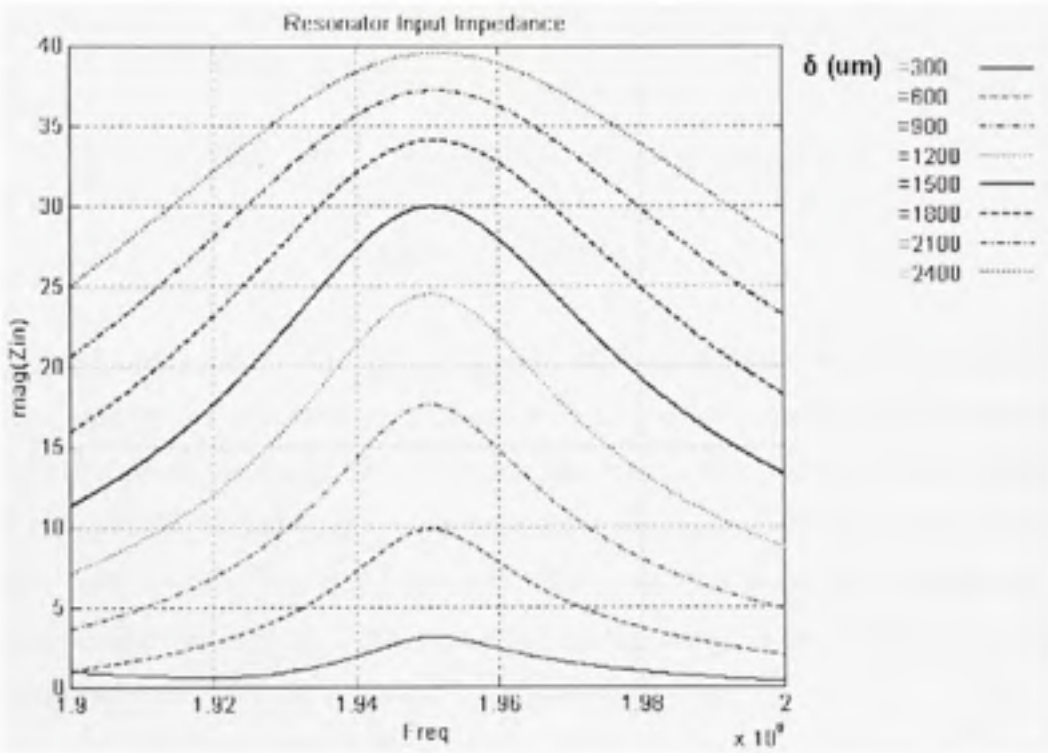

Figure 3.3 ***Magnitude of input impedance vs frequency for different values of δ.***

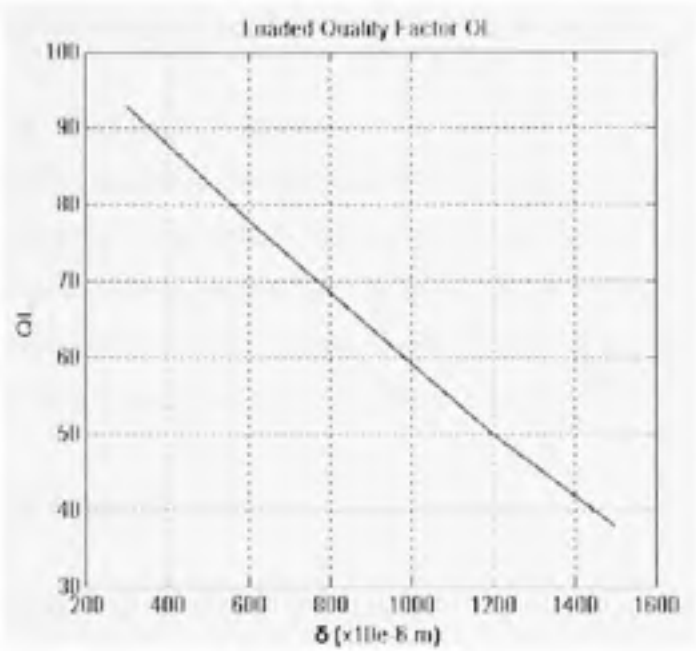

Figure 3.4 . Q_l ***vs*** δ.

From Figure 3.4 above it is clear that the loaded quality factor increases as δ approaches to zero. The variation is quite linear in general which is very convenient for tuning purposes. Figure 3.3 give us another insight into the inner-workings of this resonator: as the value of δ is decreased to achieve higher Q_l, the magnitude of the input impedance at the resonator decreases. For example, a quality factor in the order of 90 is achieved at $\delta \approx 300\ \mu m$. For $\delta \approx 300\mu$m, we find that $mag(Z_{in}) \approx 3$ at the resonance frequency, as can be seen from Figure 3.3 . Consequently a higher Q_l is achieved at a high return loss.

As we have seen in this section, the $\lambda/4 \pm \delta$ resonator allows for increasing the loaded quality factor by changing the displacement of the feed point of the resonator. And we have demonstrated that this increase is achieved at high return loss values for the resonator. In the next section we will use this resonator to design two types of second order filters. These will be the starting filter structures on which we will apply the geometrical optimisation on to achieve miniaturisation.

3.2.1 Second order band-bass filters using λ/4±δ resonators

In this section we will analyze the behaviour of two second order filter structures. We will use the electromagnetic simulation tool Momentum to analyze the response of these filters and to analyze their response to perturbations of design parameters. In general our procedure is to perform a parameter sweep for each design parameter, i.e. the parameter of interest is varied while all others are fixed. This process is repeated for each parameter, subsequently according to the obtained results the response of the filters is analysed.

3.2.2 Symmetric Feed Structure

The symmetric feed point structure is composed of two identical resonators separated by a distance X such that they are electromagnetically coupled along the length of the resonator. Moreover, the feed point for each resonator is displaced in the same direction from the mid point of the resonator as illustrated in Figure 3.5 below.

A similar filter structure to the one presented above, has been thoroughly discussed in [17]. The author in [17] demonstrated theoretically that this structure exhibits a finite frequency zero in its lower transmission band, and that the zeros are not due to cross coupling of the resonators. Rather, the transmission zeros are due to internal anti resonance in the structure. This fact is advantageous for miniaturization purposes, as it allows simultaneously, the use of only two resonators to realise a filter and the insertion of transmission zeros in the filter response. The author in [17] has used the feed lines widths' and lengths' to resolve finite frequency transmission zeros for both of these structures.

The filter structures we have started with are almost identical to the ones presented in [17], the main difference is the input feed and output transmission lines are assumed to be short and matched. This way these lines are not used in our case to resolve additional zeros or to enhance the return loss of the filter in contrast to what was done in [12]. We have imposed

this restriction on the filter structure to minimize the area occupied by the filter as a whole, otherwise the lengths of these lines would have added significantly to the size of the filter.

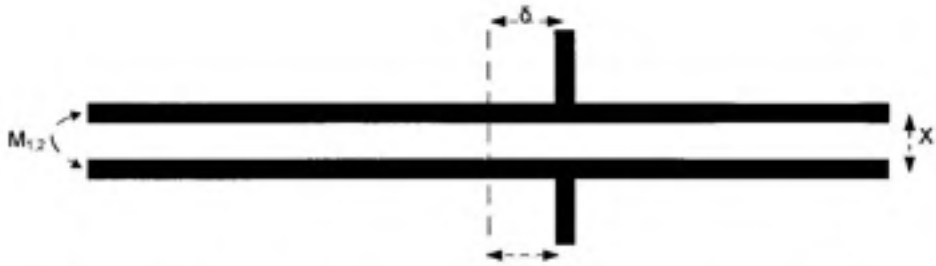

Figure 3.5 ***Second order filter using $\lambda/4 \pm \delta$ resonators in a symmetric feed configuration.***

A typical response of this filter on the MHMIC substrate of Table 3.1 is depicted in Figure 3.6. It is to be noted that the location of the transmission zero is to the low side of the pass band. The structure offers two main parameters for adjusting the response of the filter, the separation distance X and the feed point displacement from the centre δ.

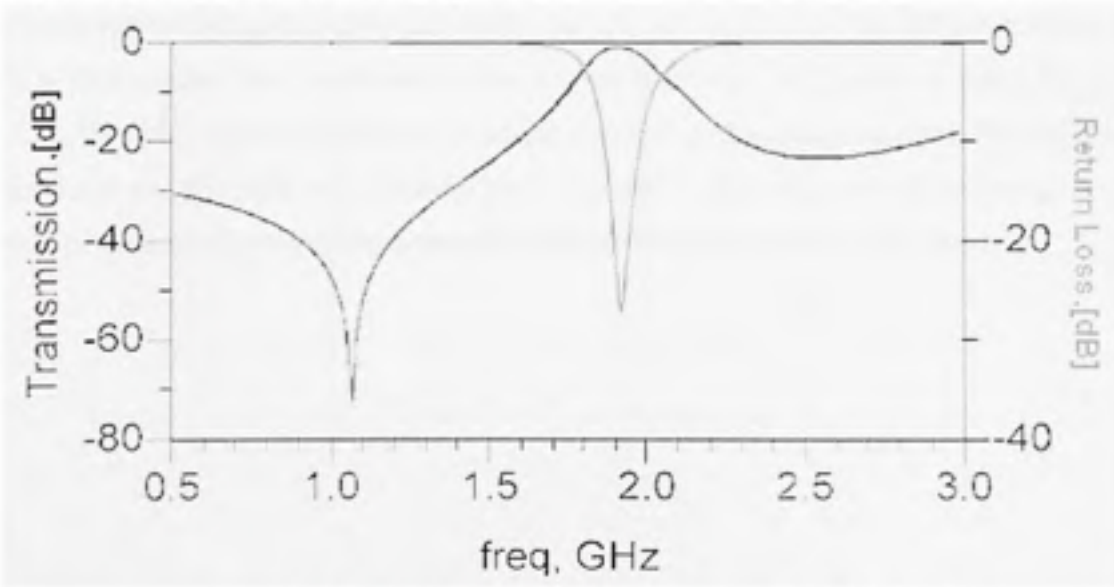

Figure 3.6 ***Typical response for the symmetric feed point filter.***

The coupling coefficient $M_{1,2}$ between the resonators is a function of the distance X between them. As this distance is decreased the coupling is increased. The effect of changing the distance X, and hence the coupling level, on the response of the filter is presented in Figure 3.7.

We are interested particularly in the following: the bandwidth of the filter, the transmission zero location, and the return loss. Although the insertion loss is a very important filter metric, it is usually closely linked to the metal thickness and conductivity accessible via a particular fabrication process, moreover in the design phase we are more concerned with the best possible topology provided we have high quality factor resonators. It is worth mentioning that the metal thickness used in the simulation is $6\,\mu m$, which is greater than twice the skin depth of gold and copper in the UMTS frequency band.

The pass band characteristic presented in Figure 3.7a indicates that as the distance between the resonators is decreased the pass band is increased measured by the 3dB attenuation point. The transmission zero is affected by the this parameter as well as can deduced from Figure 3.7c, the zero tends to displace toward the pass band, this is highly desirable effect as this produces an enhanced skirt characteristics. Figure 3.7b illustrates the return loss of the filter; it is evident that good mid band adaptation is achieved when $400 \leq X \leq 500\mu m$.

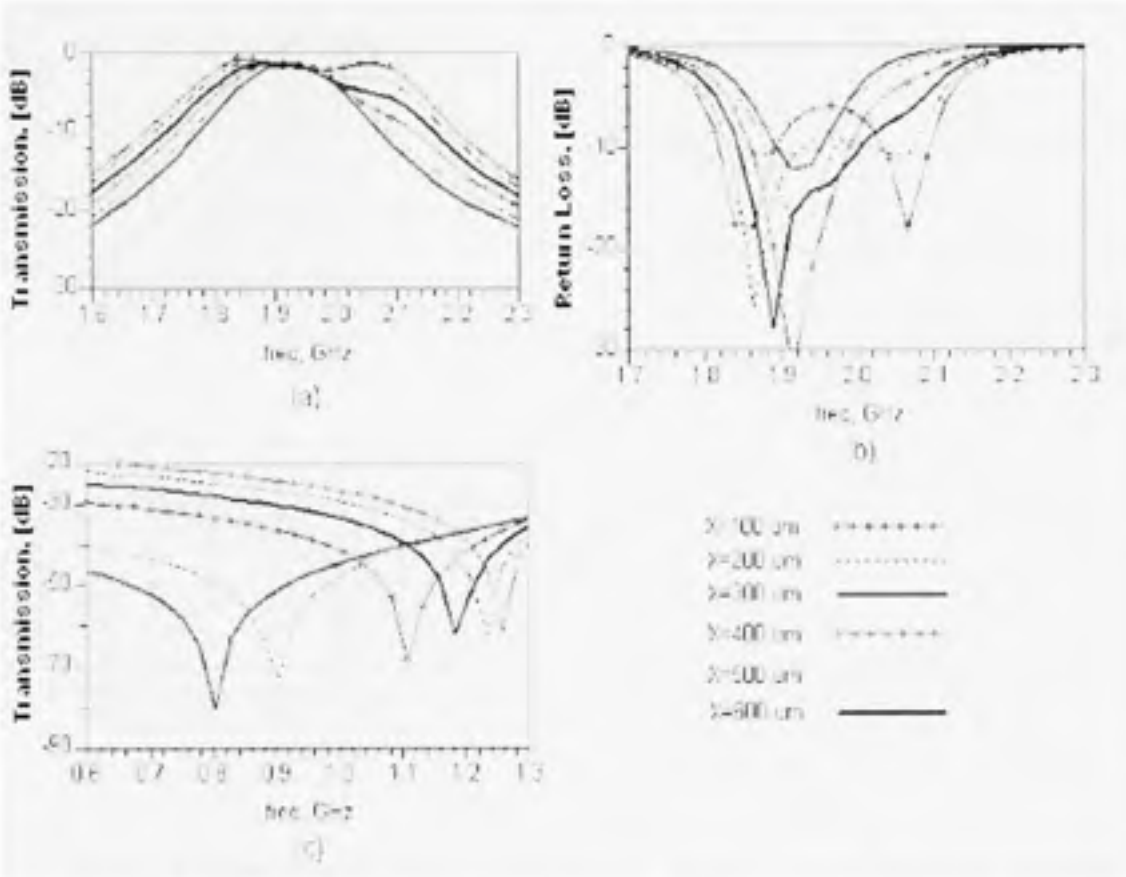

Figure 3.7 ***Effect of spacing on: transmission (a), matching (b), and zero location (c).***

The second parameter is the displacement of the feed point from the centre of the resonator denoted in Figure 3.8 by "δ". The sweep results in Figure 3.8a indicates that when the displacement is decreased the attenuation near the pass band is increased. While this is very desirable, it is unfortunately achieved at the expense of significant ripples appearing in the pass band. In addition, it is also obvious that the zero tends to approach the pass band as "δ" is decreased. The matching characteristics also show dramatic variation when "δ" is decreased below 2500 μm. This can be attributed to the increase of the loaded quality factor of each resonator to the extent that the resonators are strongly coupled only at the two split resonance frequencies.

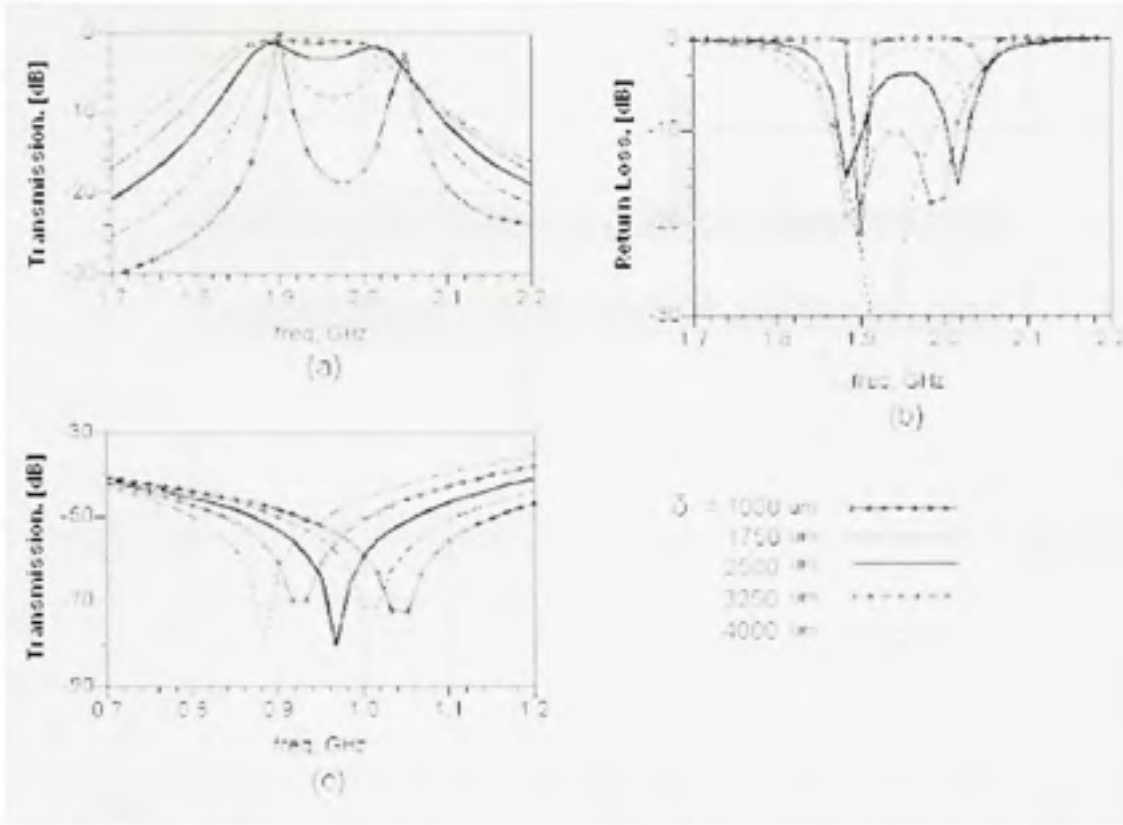

Figure 3.8 ***Effect of δ on Transmission (a), Adaptation (b) and Zero location (c).***

3.2.3 Asymmetric Feed Structure

The asymmetric feed structure is similar in construction to the symmetric structure presented above except for the direction of the feed point displacement. The feed point in this structure is displaced from the centre of each resonator in opposite directions as depicted in Figure 3.9.

This filter, in contrast to the previous one, offers its transmission zero to the high side of its pass band. A typical response for this filter, simulated using the MHMIC substrate of Table 3.1, is presented in Figure 3.10 showing the position of the transmission zero. This filter has more attractive features compared to the symmetric feed one as we will illustrate shortly.

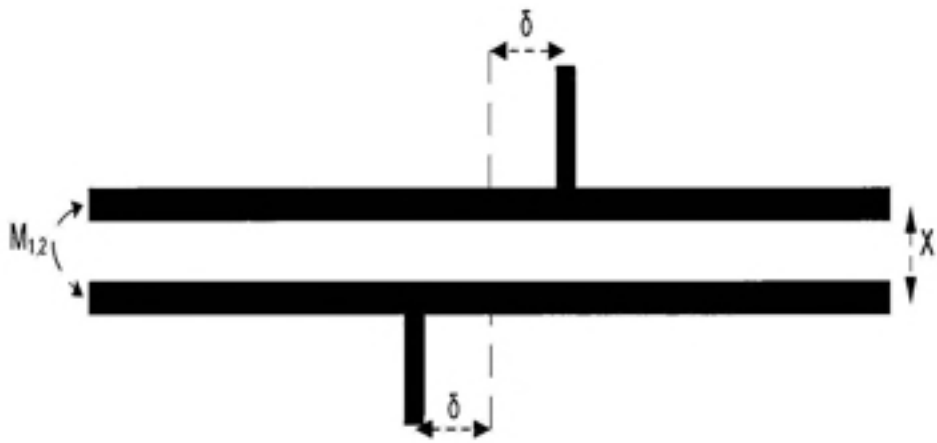

Figure 3.9 ***Second order filter using λ/4±δ resonators in asymmetric feed configuration.***

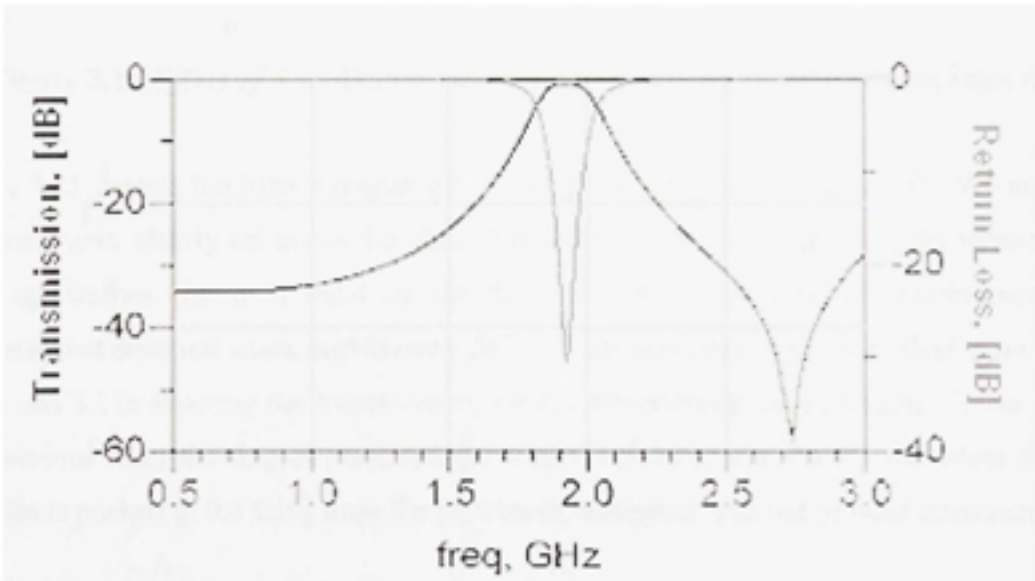

Figure 3.10 ***Typical response for the asymmetric feed point filter.***

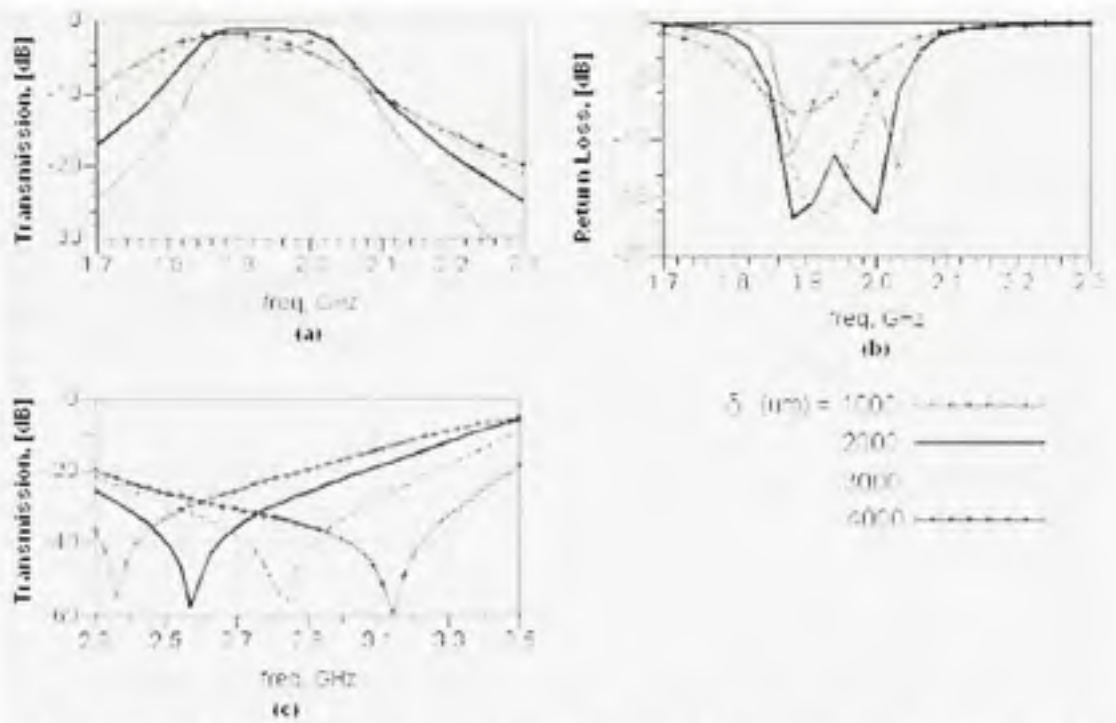

Figure 3.11 ***Effect of δ on Transmission (a), Return Loss (b) and Zero location (c).***

Figure 3.11 depicts the filter's response to varying the feed point distance "δ". We note that this parameter clearly enhances the skirt characteristics of the filter since the transmission zero approaches the pass band of the filter as "δ" is decreased. Furthermore this enhancement does not cause significant ripples in the pass band. This is evident from Figure 3.11a and 3.11c showing the transmission and the transmission zero location. In contrast to the previous filter the ripples produced are within 1.2 dB in the whole band when the zero location is pushed to 0.3 GHz from the pass band to achieve high out of band attenuation.

From Figure 3.11c we can see the variation of the input matching of the filter. The mid band matching changes significantly as a result of varying the feed point "δ". However, this variation is acceptable compared to that of the symmetric feed point structure. Finally, it is to be noted that the bandwidth of the filter is practically unchanged in response to a sweep in the feed point distance 'δ' as can be seen in figure 3.12.

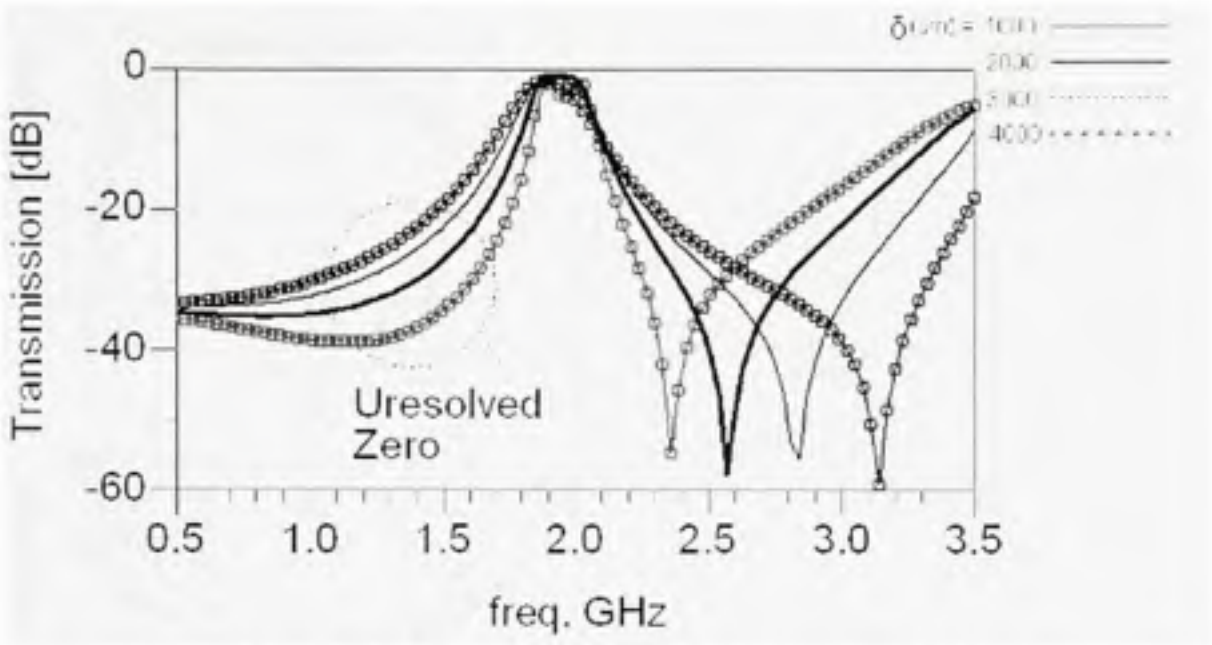

Figure 3.12 ***Effect of δ on Zero location showing an unresolved zero.***

Another highly attractive feature of this filter structure is the existence of an unresolved zero to the low side of the pass band. The unresolved zero is highlighted in Figure 3.12, where the attenuation to the low side of the pass band is dramatically improved as "δ" is decreased. This transmission zero can be resolved using the length of the feed line, however, we indicated previously, we have opted not to use this technique in an effort to miniaturise the filter. Later on, we will demonstrate another technique to resolve this zero while miniaturising the filter at the same time.

The response of the filter to the variation of the distance X between the resonators is shown in Figure 3.13. The bandwidth of the filter increases as the distance between the resonators is decreased similarly to the symmetric feed structure, but the transmission zero location hardly changes.

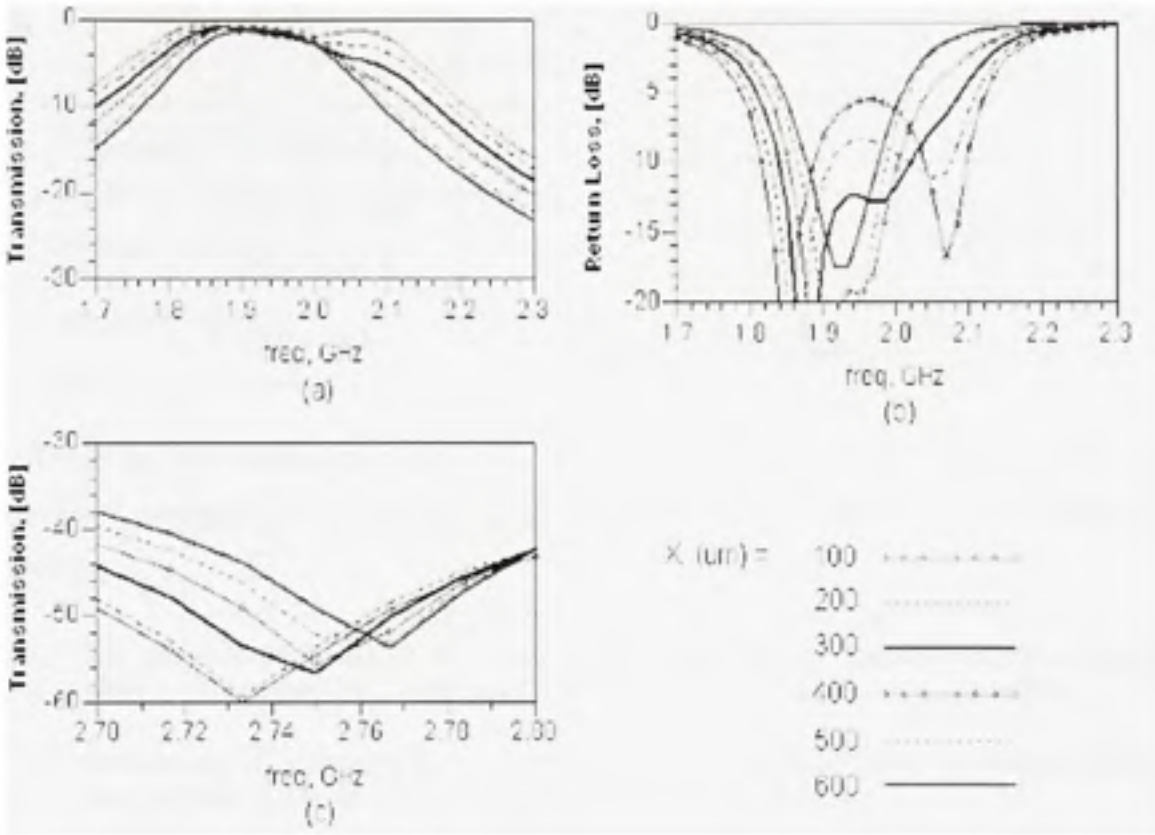

Figure 3.13 ***Effect of X on Transmission (a), Return Loss (b) and Zero location (c).***

In order to quantify the results discussed above we will numerically compare the results obtained for each parameter for the two structures: symmetric and asymmetric fed filters. For the purpose of generality we have normalised the sweep values in terms of the guided wave length for both the coupling distance X and the feed point displacement 'δ'. From the comparison of the results we will deduce which of these topologies offers further potential for miniaturization.

Table 3.3

Sweep range for filters' design parameters

Parameter	Sweep Range		
	Physical Length (μm)	Referred to λ	Electric Length[2] θ^{o}
X	100 to 600	0.0033λ to 0.02λ	0.6° to 3.6°
δ	1000 to 4000	0.033λ to 0.13λ	6° to 23.4°

In **Table 3.4** we summarize the results obtained for the presented structures. From the arguments presented above and the results presented in the Table 3.4, we observe the following:

- The variation of X has an incidence on the bandwidth for the asymmetric structure, while it affects the bandwidth and the zero location for the symmetric structure.
- Decreasing "δ" enhances the skirt attenuation for both structures, but comes with an unacceptable ripple in the pass band for the symmetric structure.
- The feed point displacement "δ" of has strong incidence on the transmission zero position and skirt characteristic and negligible effect on the bandwidth in the asymmetric structure.
- Filter return loss is sensitive to both parameters.

It is evident from the above analysis that the asymmetric structure offers better performance potential. The control over the asymmetric structure using design parameters is relatively straightforward as each design parameter mainly affects one of the performance metrics. An added feature of the asymmetric structure is the extra unresolved zero in to the lower side of

[2] The electrical length measures the physical length relative to the length of the electromagnetic wave in degrees

the bass band; a feature that greatly enhances the skirt characteristic of the filter. Consequently, the asymmetric feed structure is chosen for further study.

Table 3.4

Symmetric versus asymmetric feed response to parameter sweep

		X (μm)				δ (μm)			
		Min		Max					
		100		600		1000		4000	
Metric		Sym.	Asym.	Sym.	Asym.	Sym.	Asym.	Sym.	Asym.
Bandwidth	Absolute *MHz*	333	342	130	154	154	168	186	158
	Fractional %	16	**17.6**	6. 5	**7. 7**	7. 7	8. 4	9. 3	7.9
Transmission zero freq. *GHz*		1. 25	2.734	0.8	2.766	1.0	2. 37	0. 88	3. 138
Skirt attenuation[3] *dB*		7	8	9	8	23	**14.6**	8	**5**
Return loss *dB*		-6	-5.7	-20	-18	-0.1	-3. 3	-25	-7.7

3.2.4 Topological Optimization

In the previous section we have chosen the asymmetric filter structure for further optimization. The technique of topological optimisation was introduced in [8] and applied to a square filter topology. It consists of finding a more compact topology using electromagnetic simulation and heuristic optimisation. Although this technique is difficult and time consuming, especially in the early phases of the design, it results in compact filters with excellent performance as demonstrated in [8] and in this current work. One of the difficulties with the topologies introduced in [8] is that there is no clear methodology for

[3] The attenuation is evaluated at 100MHz from the 3dB point

miniaturisation. The structures are miniaturised using the sections' lengths and widths at the same time. Another difficulty is that the length of the final resonator is longer than half the guided wavelength, which violates the initial assumption that the structure is half wavelength-based. As a result of the excessive length of the resonator it was necessary to fold it many times while successively reducing the width of the transmission line. These difficulties resulted in complex coupling and geometry. It also gives little insight into how to achieve similar results using their technique.

Our approach to topological optimisation is to fold the arms of the resonators previously introduced while keeping the asymmetrical structure unchanged. The maximum number of folds we use is two. Also, in our technique, the overall length of the resonator remains half the guided wavelength. Furthermore, the width of the transmission line is not used except for fine tuning of the filter at the end of the design cycle. Coarse tuning is achieved through varying the transmission line width. It is the simplicity of this technique which makes it relatively easy to develop a topology that achieves good performance in a significantly miniaturised size.

The topology depicted in Figure 3.14 is the result of a single fold operation. Its typical frequency response is presented in Figure 3.15. It is evident that the transmission zero to the lower side of the passband has been resolved as required and that the filter has excellent attenuation properties. At this point it is important to ensure that our basic design parameters are acting in the same way as in previous structures.

The results presented in Figure 3.16 demonstrate that design parameters affect this structure generally in the same way as in the unfolded asymmetric feed point structure. Despite satisfactory transmission and attenuation the size of the filter is still relatively large approximately $14.7\,mm$ x$4.7\,mm$ which is equivalent to $0.5\,\lambda$ x$0.15\,\lambda$. In performance terms the return loss of the filter is still limited as does not exceed -10dB in the middle of the pass band.

Figure 3.14 ***First iteration of topological optimisation.***

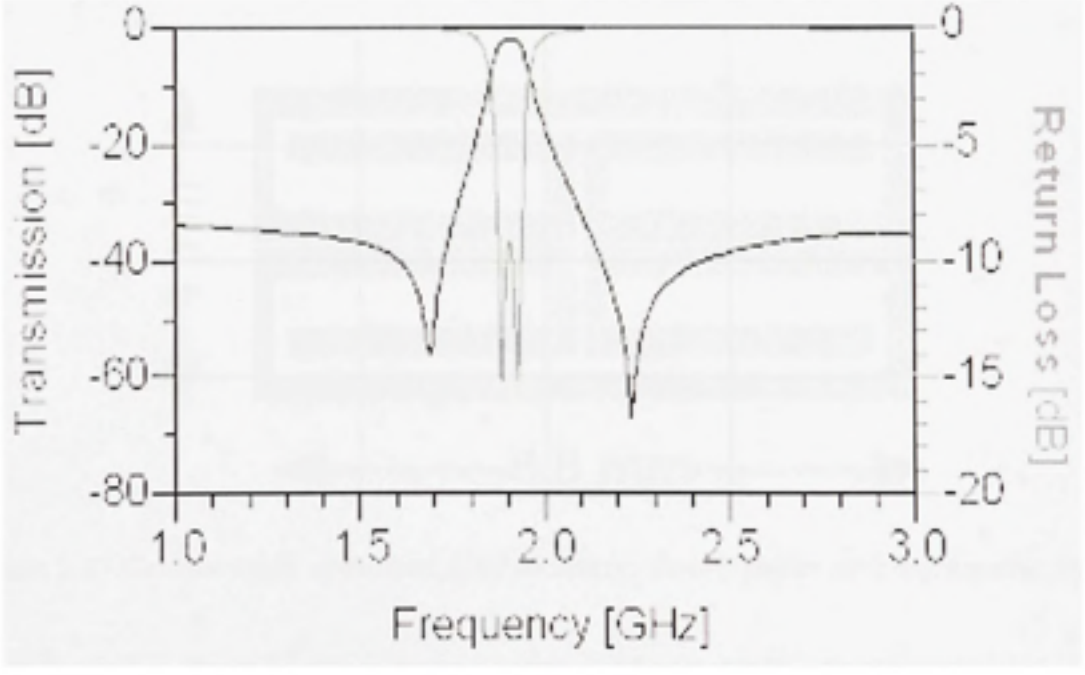

Figure 3.15 ***Transmission and return loss response of the topology in Figure 3.14.***

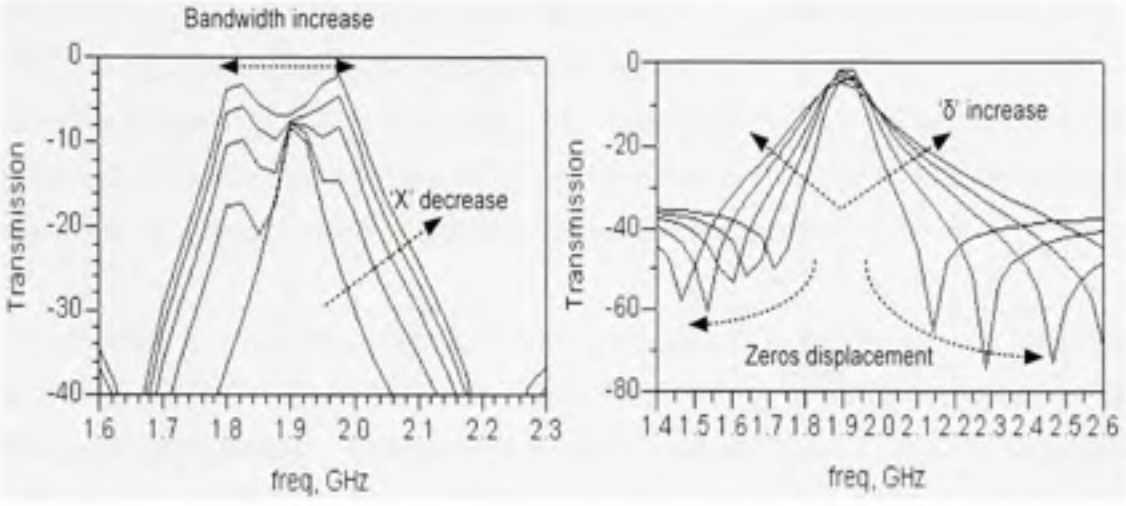

Figure 3.16 ***Response of the filter as a function of design parameters sweep.***

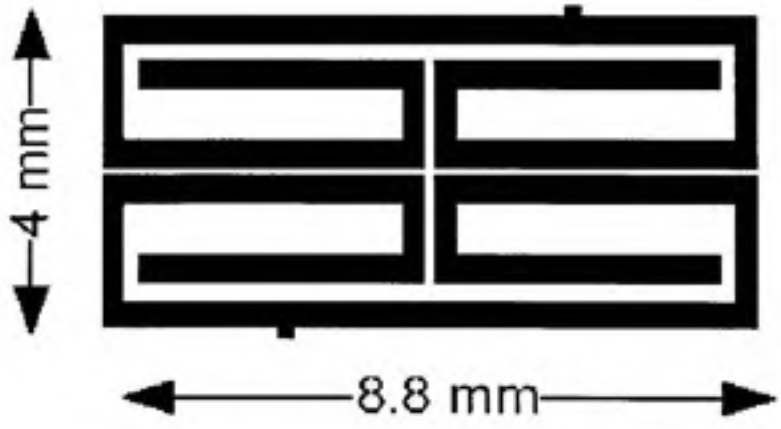

Figure 3.17 ***Geometrically optimized filter structure: doubly folder with asymmetric feeds.***

Using the same miniaturisation technique we proceed with folding the filter arms to achieve further miniaturization of the structure. The resulting structure is depicted in Figure 3.17, the size of the structure is now reduced by almost 50% to 0.06λ x0.14λ. The internal arms of this structure provide additional paths between the input and output of the filter. These paths

have resulted in an additional zero in the filter response as highlighted in the figure 3.18. It is clear that the attenuation characteristics to the high side of the pass band, where the extra zeros are located, are greatly enhanced. This performance enhancement has come with a price, namely a difficulty in finding the optimal solution and a difficulty of maintaining good return loss for a given bandwidth and skirt attenuation requirements.

The difficulty in maintaining suitable return loss stems from the fact that the return loss is sensitive to both our design parameters the separation distance between resonators and the feed point displacements. This problem has been illustrated earlier when we presented the basic filter structures in section. In the next section we present a structure that offers an additional degree of freedom for adjusting the return loss.

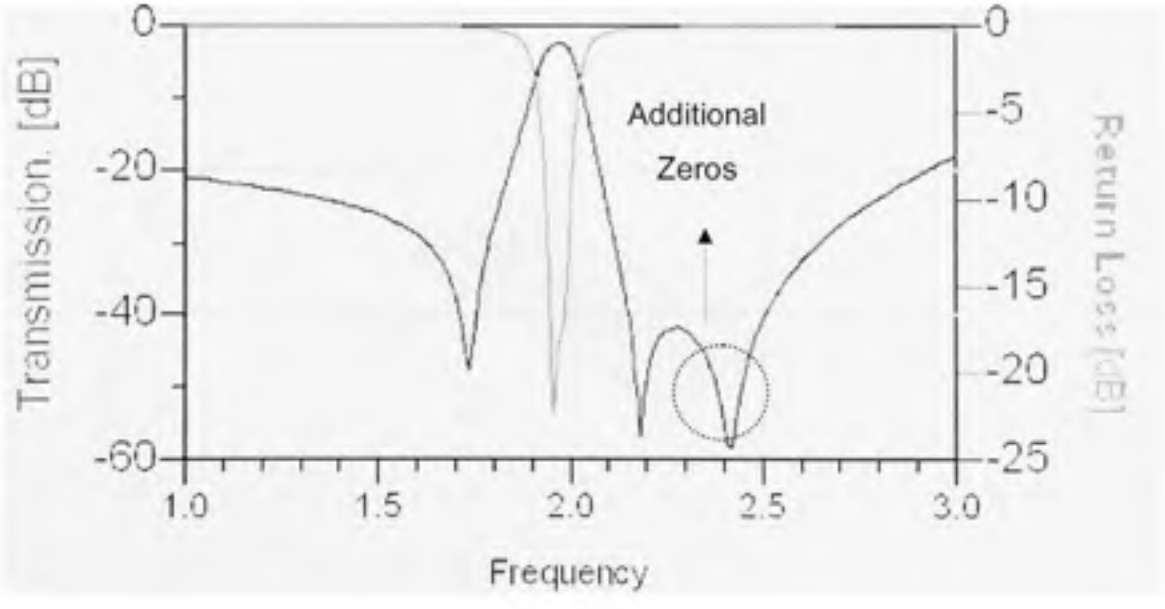

Figure 3.18 ***Transmission and return loss response of the topology in*** **Figure** ***3.17.***

3.2.5 Modified port structure

The return loss of the miniaturized structure suffers from poor controllability, which stems from return loss sensitivity to design parameters. This results in reduced degrees of freedom per performance metric. In order to better understand the problem and the structure we have constructed a three dimensional model (Figure 3.19) of the miniaturized structure using EMDS[4] to analyse the flow of energy in the structure. In three dimensional electromagnetic modeling and simulation, it is very important for the accuracy and validity of the results to reach a mesh that properly captures the variation of the electromagnetic field at the desired frequency. We have used the adaptive mesh refinement utility available in EMDS which enables us to progressively achieve a good mesh. A mesh is considered good when a good compromise between the memory and accuracy requirements has been attained.

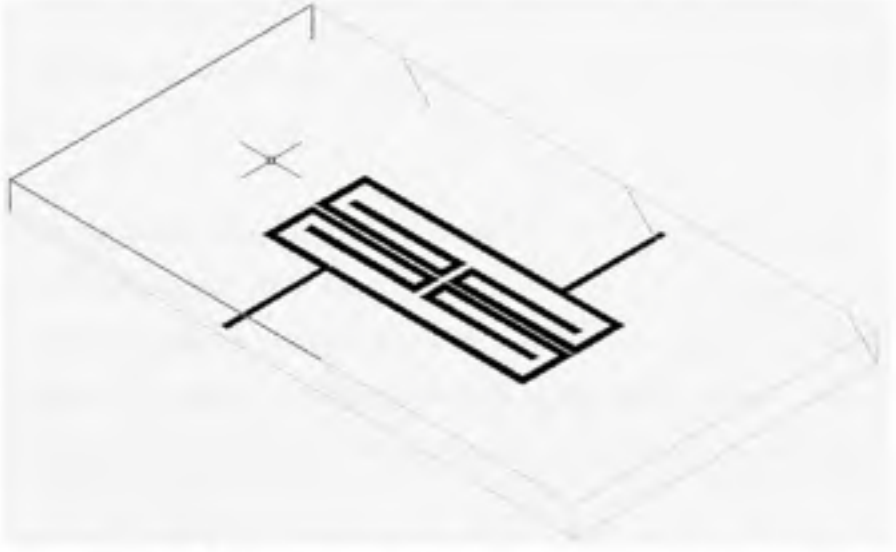

Figure 3.19 ***3-Dimensional doubly folded filter model in EMDS.***

[4] EMDS is a three dimensional model capture and electromagnetic simulator provided by Agilent

In order to insure that our Momentum simulation (2.5D) captures properly the physics of our structure we have compared it to the 3D model simulation results obtained from EMDS. The comparison is depicted in Figure 3.20. We notice that excellent agreement between the two models is obtained. These results give us confidence that the 2.5D simulation obtained through Momentum is good compromise between the simulation time and accuracy.

Once the three dimensional model is properly meshed and simulated we used the postprocessor engine to calculate and display the poynting[5] vector to analyse energy flow in the filter structure. The mesh and the poynting vector distribution are shown in figure 3.21. From this figure we can see that the poynting vector's intensity is maximum in the folded arms next to the gap between the resonators. We also note that the return loss problem lies in the inefficient port structure that has a low energy transfer as indicated by small arrow size in the right figure. This has led us to conclude that, in order to improve the filter return loss, we need to find a better port structure to couple energy more efficiently to the internal arms of the resonators.

To the end of better return loss, we propose to modify the port structure as shown in figure 3.22. Instead of the standard 50Ω transmission line feed, we introduce a small section of lower characteristic impedance transmission line, i.e., a section with a wider line. To asses the impact of this line's width, i.e. the parameter Y, on the filter response we proceed with a parametric study similar to the previous ones conducted on resonator spacing and feed offset.

---

[5]Poynting vector is calculated from the electric and magnetic fields as follows: $\bar{S}=\frac{1}{2}\bar{E}\times\bar{H}^*$ where $\bar{S}$ is the apparent or complex power

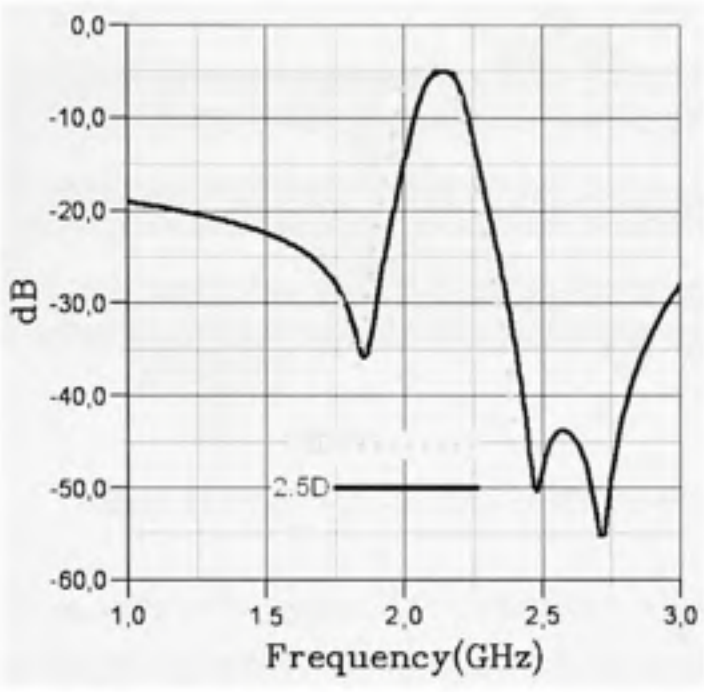

Figure 3.20 ***Momentum (2.5D) vs EMDS (3D) simulation results.***

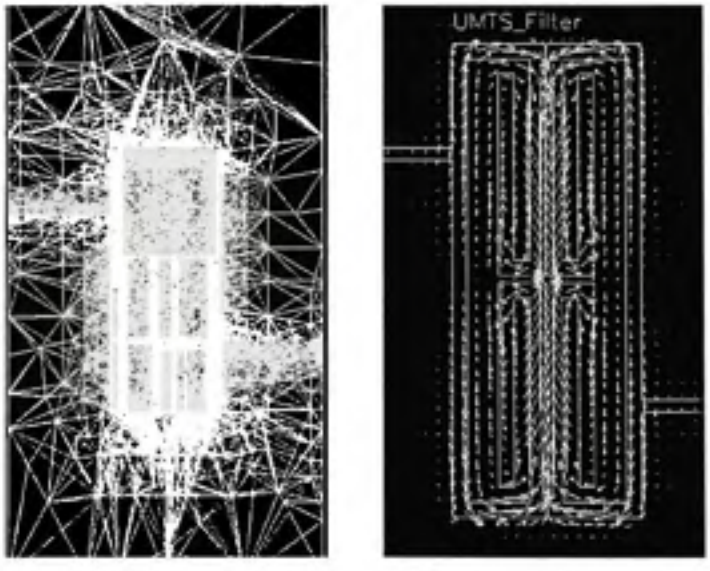

(a) Model mesh **(b) Poyting vector distribution**

Figure 3.21 ***(a) the mesh used (b) the Poynting vector distribution at 1.96GHz.***

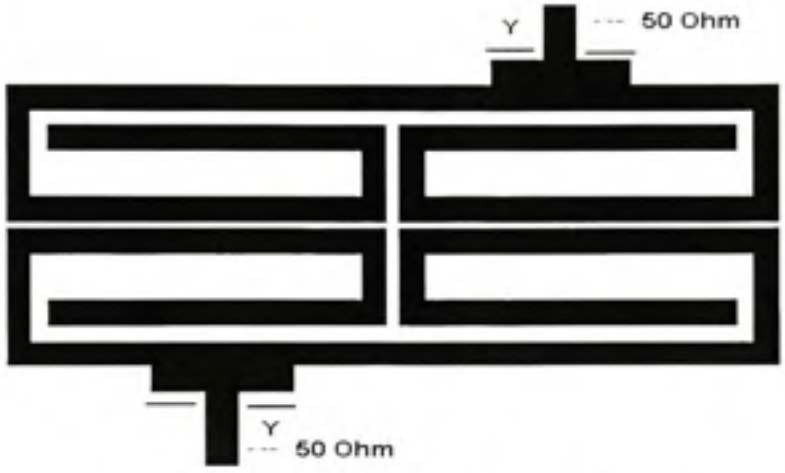

Figure 3.22 ***Filter topology with modified ports.***

The result of a sweep study of the parameter Y is presented in Figure 3.23. We observe through this figure that varying the line width can improve the return loss while having minor effect on the center frequency of the filter. Indeed, for Y= 800 μm the mid band return loss is below -16dB, which represent an improvement of more than 3dB compared to the standard (Y=0) case. We also note that the centre frequency is shifted to the right as Y is increased. This effect can be compensated by designing the filter at a slightly lower center frequency or by adjusting the length of the internal arms of the filter.

In general we can say that the introduced parameter "Y" has successfully produced the desired effect of enhancing the return loss of the filter without adverse effects on its other metrics. Consequently the degrees of freedom for this topology are increased, allowing more design flexibility.

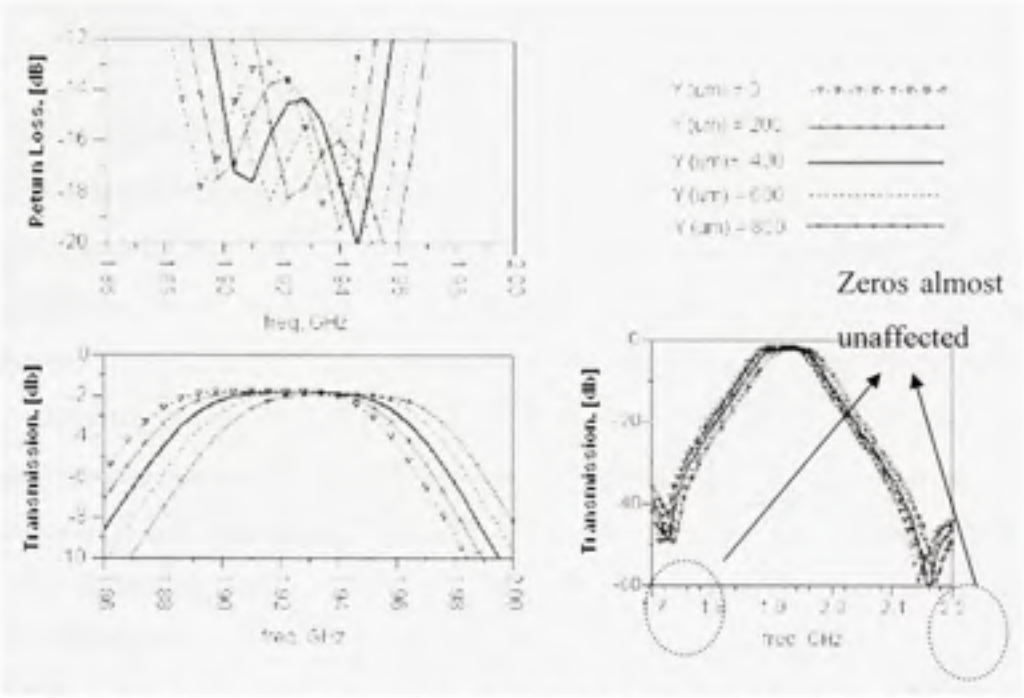

Figure 3.23 ***Filter response to variation of port width (Y) for the topology in Figure 3.22.***

To illustrate the new design technique, an optimized receive band filter for UMTS user terminal profile is designed and its response is presented in Figure 3.24. The attenuation in the middle of the transmission band, at 1.94GHz, is -33dB and the insertion loss is -2.36 dB while the return loss is better than -15dB. The size of this filter is 3.9mmx9.2mm which is 40% smaller than filters reported in [8].

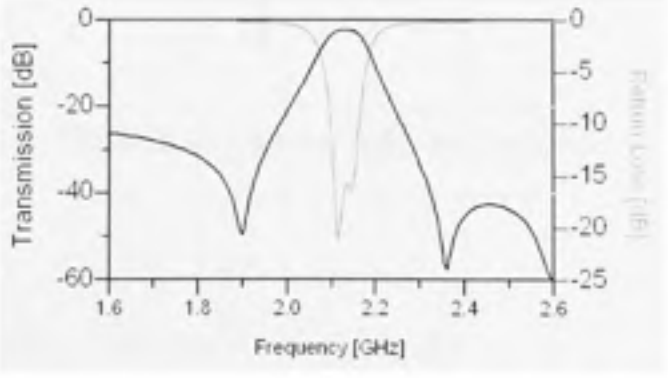

Figure 3.24 ***Filter response of the topology in Figure 3.22.***

3.3 Design of miniaturised duplexers

The design of duplexers is straight forward once we have designed the miniaturised filters. A duplexer using the miniaturized filters was designed using two $\lambda/4$ impedance transformers, each transformer lies between its respective filter and the antenna, figure 3.25. In addition to the transformer there is a T-junction that connects the antenna to both impedance transformers. The duplexer topology was optimised similar to the filters by meandering of the $\lambda/4$ transformers such that the total size of the duplexer is reduced, figure 3.26. The size difference between the classical duplexer and the optimised one is about 30% size reduction, and compared to the duplexer presented in [8] is about 14% reduction in size. figure 3.27 shows the electromagnetic simulation results of the designed filter using the MHMIC substrate of table 3.1.

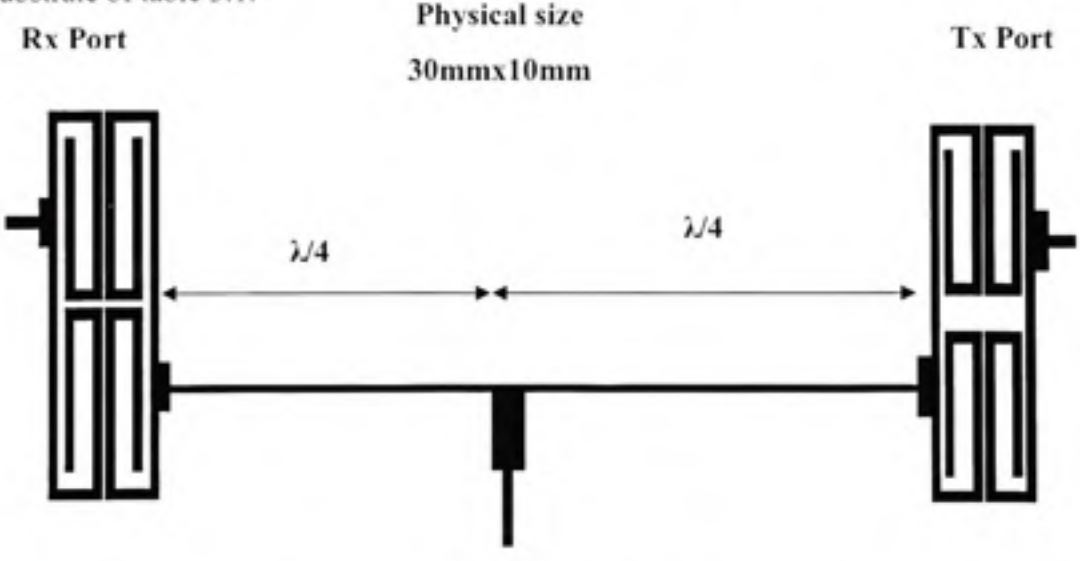

Figure 3.25 *Classical duplexer structure.*

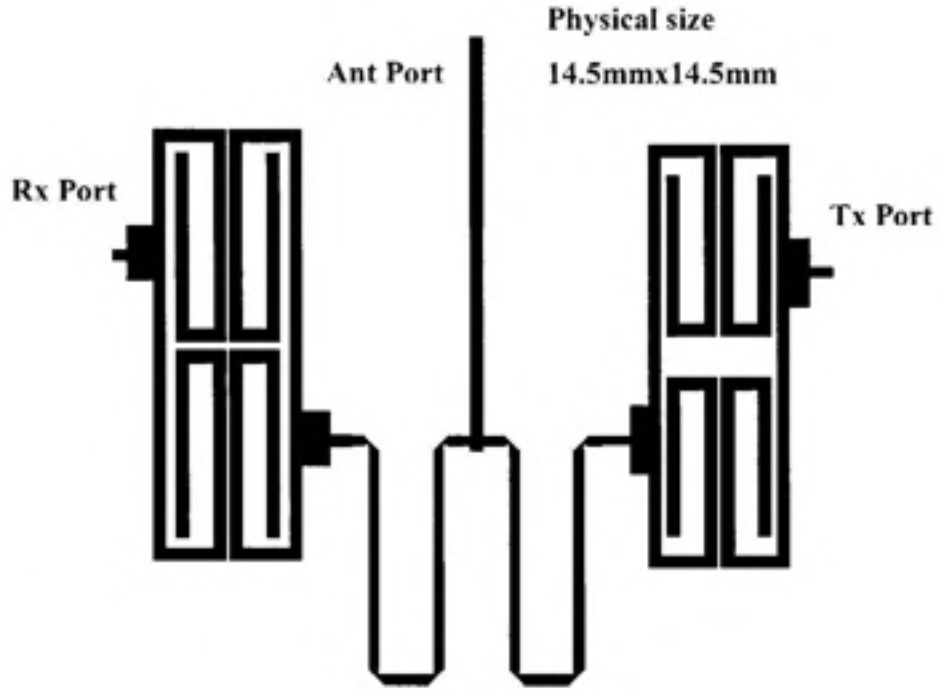

Figure 3.26 ***Topologically optimized duplexer structure.***

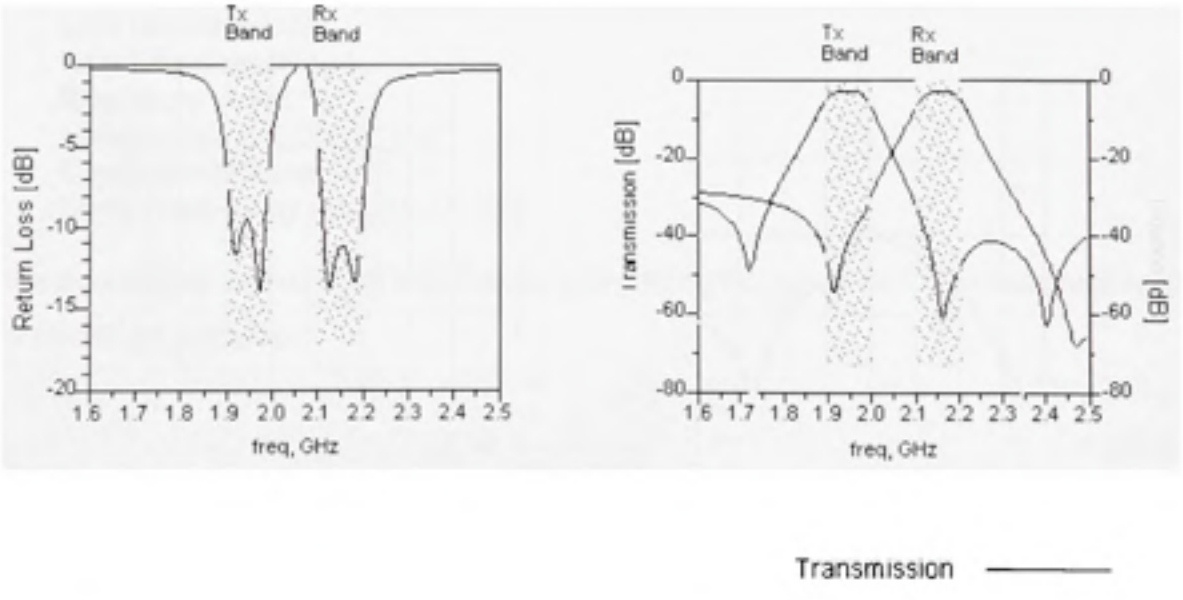

Figure 3.27 ***Optimised duplexer response (Left) Return loss, (Right) Transmission.***

This set of results demonstrates excellent performance and miniaturization when compared to the state of the art in the field.

3.3.1 Fabrication results on MHMIC process

3.3.1.1 Introduction

In this section we will present the measured results following fabrication of the filters and duplexers that were designed using our proposed technique using a MHMIC process substrate. All fabricated filters and duplexers were measured using the Wirltron fixture kit to avoid packaging the circuits and adding connectors to them. Measurements were taken using the Agilent Vector Network Analyser after a TRL calibration procedure [18]. The MHMIC substrate used in the fabrication process has the following properties:

Substrate thickness10 mil +/- 5%
Relative permittivity (ε_r) 9.9
Loss tangent 0.0001
Relative permeability 1
Roughness ~1 µm
Maximum circuit size .9" x .9"
Conductor thickness 1 µm
Metal conductivity (Gold) 4.1e7 S/m

We can estimate the mid band filter loss theoretically on this substrate for the frequency band of interest by applying

$$Q_u \approx \frac{\pi}{2\alpha(l_- + l_+)} \tag{3.1}$$

and the following equation from [19]:

$$IL = \frac{4.34 f_0 \sum_1^n g_i}{\Delta Q_u} \tag{3.3}$$

Where g_i 's are the low pass filter parameters. Although our filter is not derived from a low pass prototype we can estimate the g_i values. We know from classical Chebychev filter tables that g_i are usually in the range of 0.6 to 0.82. Taking an average between these values and considering that we target band pass filters of relatively low fractional bandwidth between 2% to 4%, we estimate that the insertion loss at mid band to be between 3.7 to 5.0 dB. Most of the loss is due to conductor losses arising mainly from metal layer thickness. One of the main limitations of this particular fabrication process is that higher metal thicknesses are not available, causing a poor resonator quality factor and consequently high loss.

3.3.1.2 First Fabrication Run

The filter specifications targeted for this run are in the 5GHz band and are as follows:

Pass Band for Transmission Filter: 5.15GHz to 5.35GHz

Pass Band for Reception Filter: 5.55GHz to 5.75GHz

Insertion Loss: 3dB

Tx Filter Attenuation @ Rx Band (5.55GHz): 30dB

Rx Filter Attenuation @ Tx Band (5.35GHz): 30dB

It is important to mention that the in the band of interest a quarter wave length line is approximately equals to 5.5mm. This makes our basic resonator's length equals 11mm.

First, pair of transmission and reception filters was designed. Then a duplexer was realised based on these filters. The photographs of the fabricated filters and duplexers are shown Figure 3.28.

Figure 3.28 ***(Left) Filter (Right) Duplexer.***

The measurements results of for the transmission side filter of the transmission filter of the duplexer is presented in Figure 3.29 and Figure 3.30, while the measurements results for the duplexer a s a whole are presented in the Figure 3.31. In general we note good agreement between simulation and measurements, except for the receive side of the duplexer. The difference witnessed for the receive side of the filter is due to that the receive filter had smaller spacing than the fabrication process precision. This caused the fabricated filter to have tighter spacing than the simulated causing excessive coupling between the resonators.

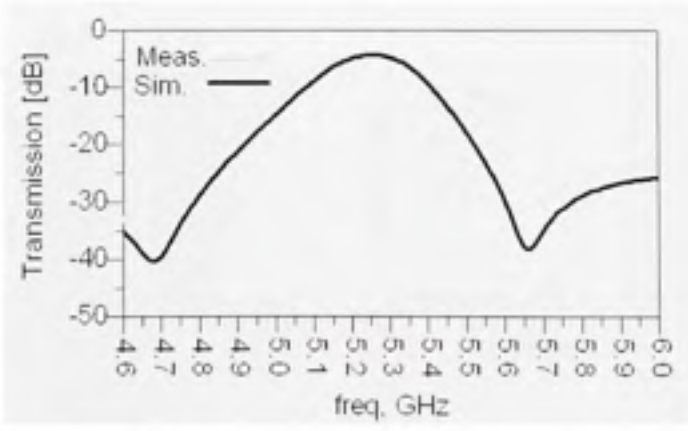

Figure 3.29 ***Filter measurements (Transmission).***

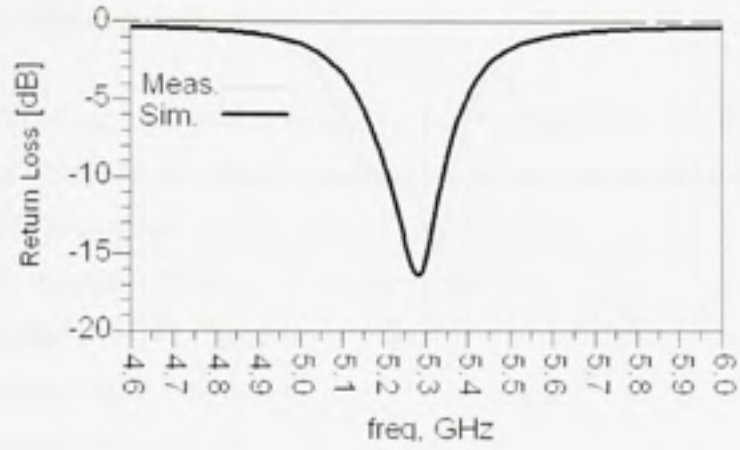

Figure 3.30 ***Filter measurements (Return loss).***

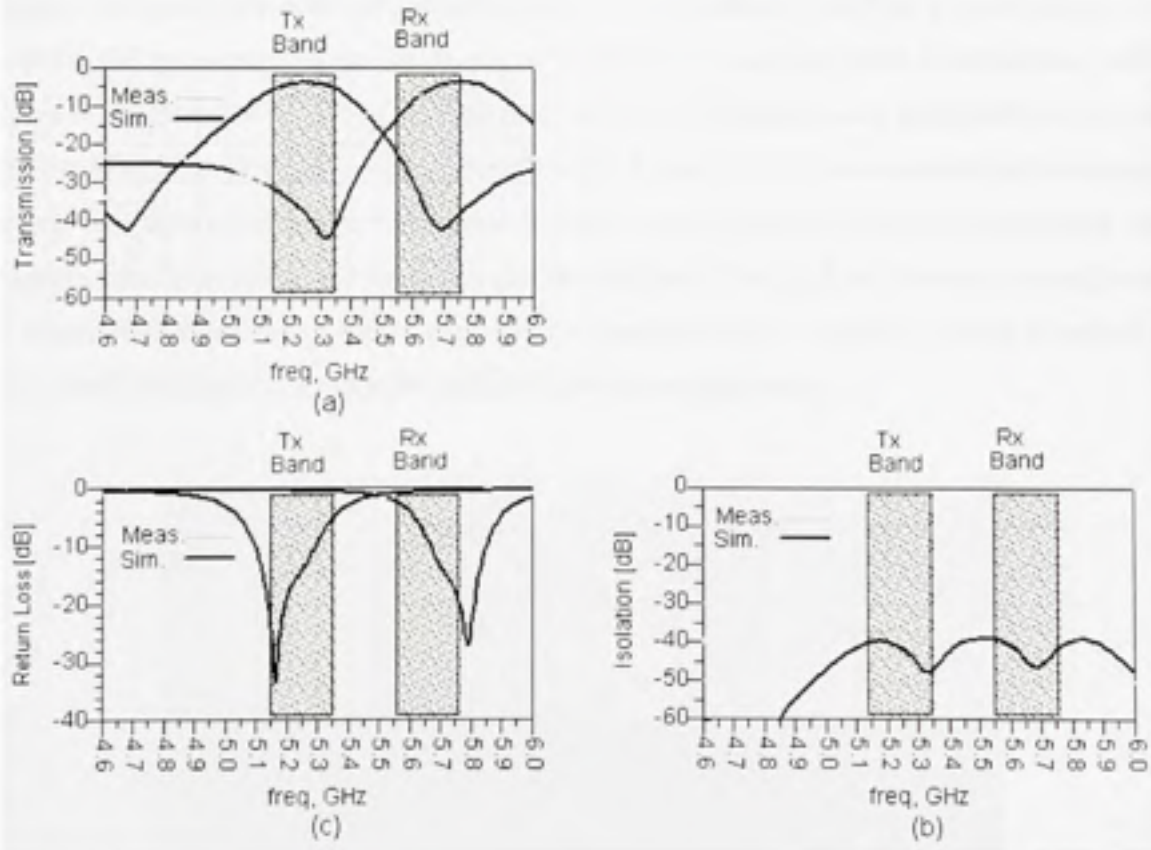

Figure 3.31 ***Duplexer, Transmission (a), Isolation (b) and Return loss (c).***

3.3.1.3 Second Fabrication Run

In the second fabrication run we have targeted a UMTS filter duplexer profile. The typical requirements for a UMTS filter duplexer for mobile terminals are as follows:

Pass Band for Transmission Filter: 1.92GHz to 1.98GHz

Pass Band for Reception Filter: 2.11GHz to 2.170GHz

Tx-Antenna attenuation (Tx-band) <2

Rx- Antenna attenuation (Rx-band) <3

Tx-Rx isolation (Rx-band) >37

Tx-Rx isolation (Tx-band) >50

Figure 3.32 shows the fabricated transmit and receiver filters for the UMST band. figure 3.33 presents the measured results for the transmit filter and compares them to simulation while figure 3.34 presents a similar comparison between simulation and measurement for the receive filter. The fabricated duplexer is shown in figure 3.35 and its measured and simulated results are shown in figure 3.36. Overall, very good agreement between simulation and measurement is observed for the filters and the duplexer. The slight differences are attributed to some effects that are not fully captured by electromagnetic simulation, such as radiation loss, metal thickness modeling and effect of the measuring fixture.

Figure 3.32 ***UMTS filters topologies. (Left) Tx-filter (Right) Rx-filter***

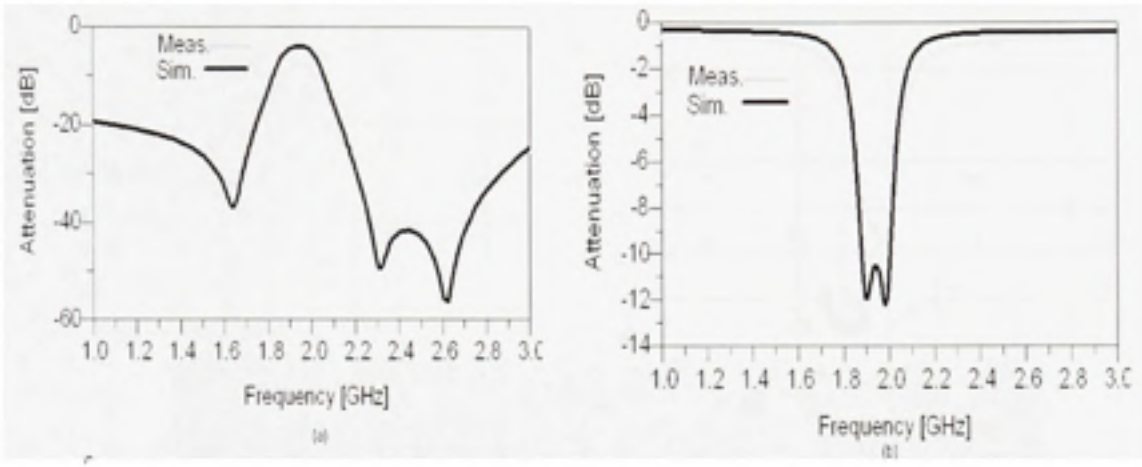

Figure 3.33 ***UMTS Tx- filter fabrication, Transmission (a), Return loss (b).***

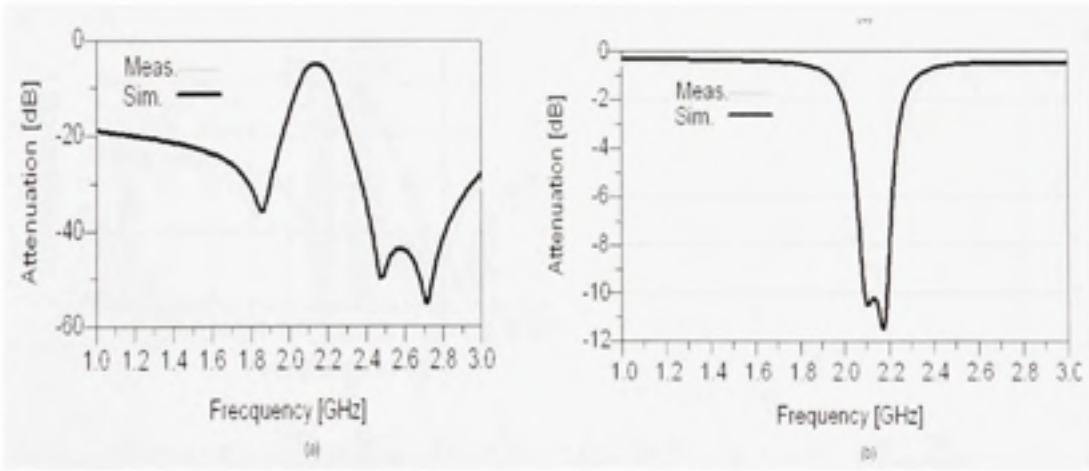

Figure 3.34 ***UMTS Rx filter fabrication Transmission (a), Return loss (b).***

Figure 3.35 ***UMTS duplexer topology.***

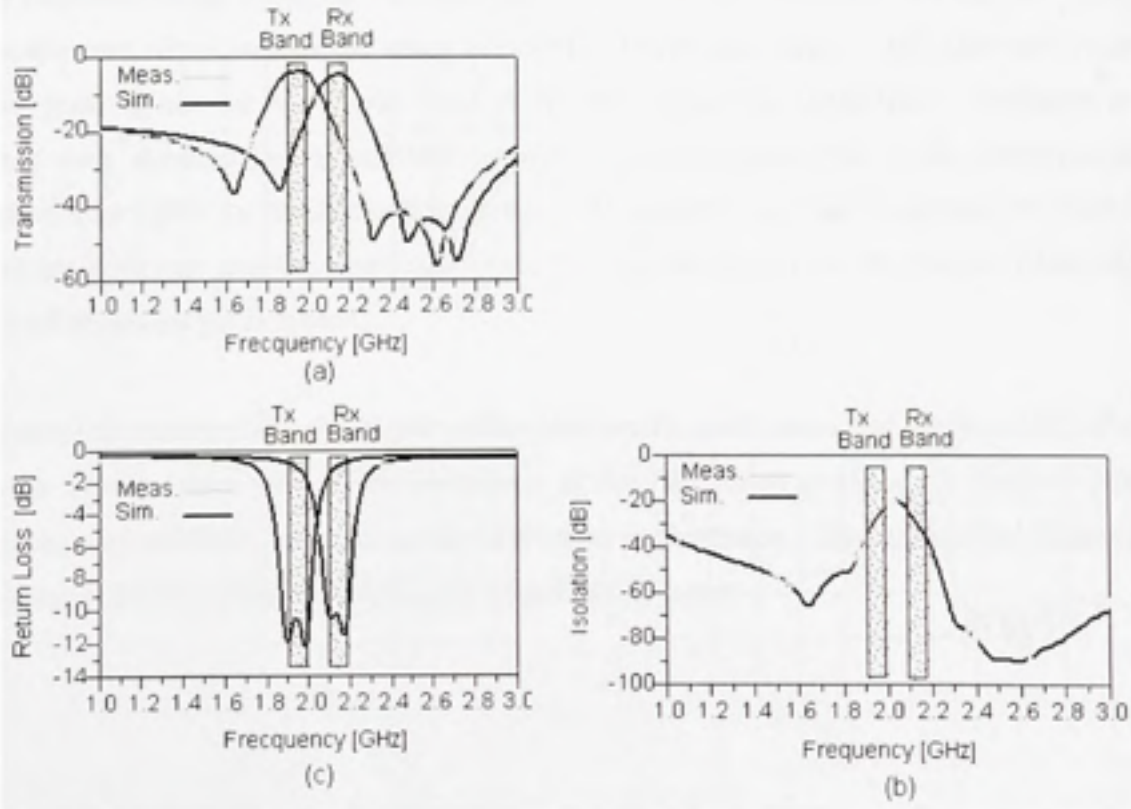

Figure 3.36 ***UMTS Duplexer fabrication: Transmission (a), Isolation (b) Return loss (c).***

3.4 Conclusion

In this chapter we have introduced the methodology developed for designing miniaturised filters and duplexers. We have also introduced a new topology that provides transmission zeros above and below the pass band of the filter. The final structure highly simplifies the design of these filters because the design parameters are decoupled from all but one performance metric. The proposed methodology for designing high quality filters using the proposed structure is to control the bandwidth of the filter using the resonator spacing parameter (X), then to tune the position of the transmission zero using the offset feed parameter (δ) and finally to adjust the return loss of the filter using the feed line width parameter (Y). This technique was shown to produces highly compact filters with very attractive filtering characteristics.

The proposed design technique has been applied to realise several filters and duplexers pairs on a standard Alumina substrate using an MHMIC fabrication process. Measurement results show good agreement with those obtained by electromagnetic simulations. Although the losses were elevated for the MHMIC process, it was expected due to the limited metal thickness available in the fabrication process. In addition, the high tolerance (+/-5%) in substrate thickness and the sensitivity of the filter to this parameter resulted in a less than optimal measured performance.

Although the results show significant miniaturization, the performance of the filters is limited by the Ohmic losses due to the limitations of the fabrication process. A more evolved process, such as MMIC process, could offer better performance. The next chapter discusses the development of filters and duplexers on a MMIC process.

CHAPTER 4

FILTERS AND DUPLEXERS IN MMIC TECHNOLOGY

4.1 Introduction

In the chapter we will present the design of miniaturised filter based on MMIC process. The target process is the TQPED process provided by TriQuint Semiconductors. The TQPED is a pHEMT process on which active components and high quality factor passives can be integrated. MMIC processes are different from one manufacturer to another but typical substrate parameters and stack-up are given in the Table 4.1.

Table 4.1

Typical stack up of a MMIC substrate

Layer	Material	Function	Thickness (μm)	Relative Electric Permittivity	Electric Conductivity (S/m)	Loss tangent
0	Copper	Ground	-	-	5.8e7	-
1	GaAs	Substrate	254	12.9	-	0.0001
M0	Aluminium	Metallization	0.4	-	2.9e7	-
ILD1	Insulator	Inter Layer Dielectric1	1	2.8	-	-
M1	Gold	Metallization	2	-	4.1e7	-
ILD2	Insulator	Inter Layer Dielectric2	3	2.8	-	-
M2	Gold	Metallization	4		4.1e7	-

This process provides better features for possible filter design such as, a high dielectric constant of 12.9 which is good for high miniaturization, a highly precise metal deposition techniques, which allows for less spacing between features and the possibility of connecting all metal layer together using stacked VIAs to obtain a metal thickness of as much as 6.4μm

leading to better unloaded quality factors. In table 4.2 we note that the quarter wavelength of the transmission line is smaller than that obtained for MHMIC substrate of table 3.1. However, it is not clear if this will be sufficient to realize very small-size distributed filters and duplexers.

Table 4.2

Geometrical and electrical characteristics of a transmission line

Electrical		Geometrical	
Characteristic impedance Z_0 (Ω)	50	Width (μm)	181
Electrical length (Deg.)	90°	Length (μm)	13100

4.2 Coupled resonator filter design

The procedure for designing the filter was introduced in previous chapters, consequently only the main results will be presented here. A filter for the UMTS transmission band was designed using a simplified stack-up of the substrate for the purpose of space evaluation. Figure 4.1 shows the topology of the designed filter, while figure 4.2 presents the electromagnetic simulation results of this filter.

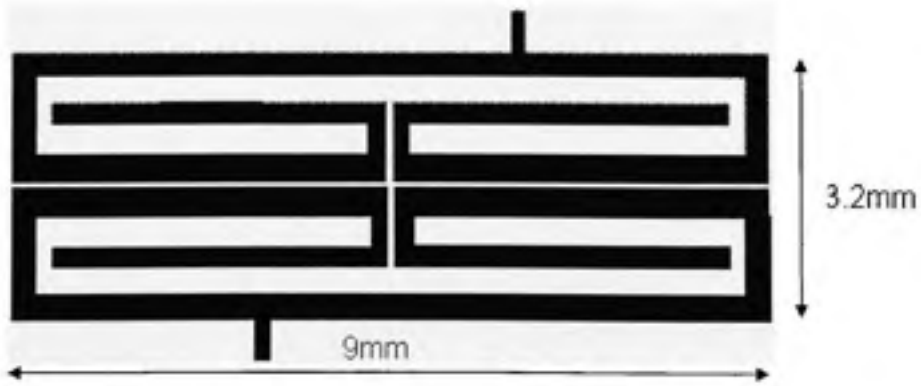

Figure 4.1 ***Preliminary coupled resonator filter on MMIC substrate.***

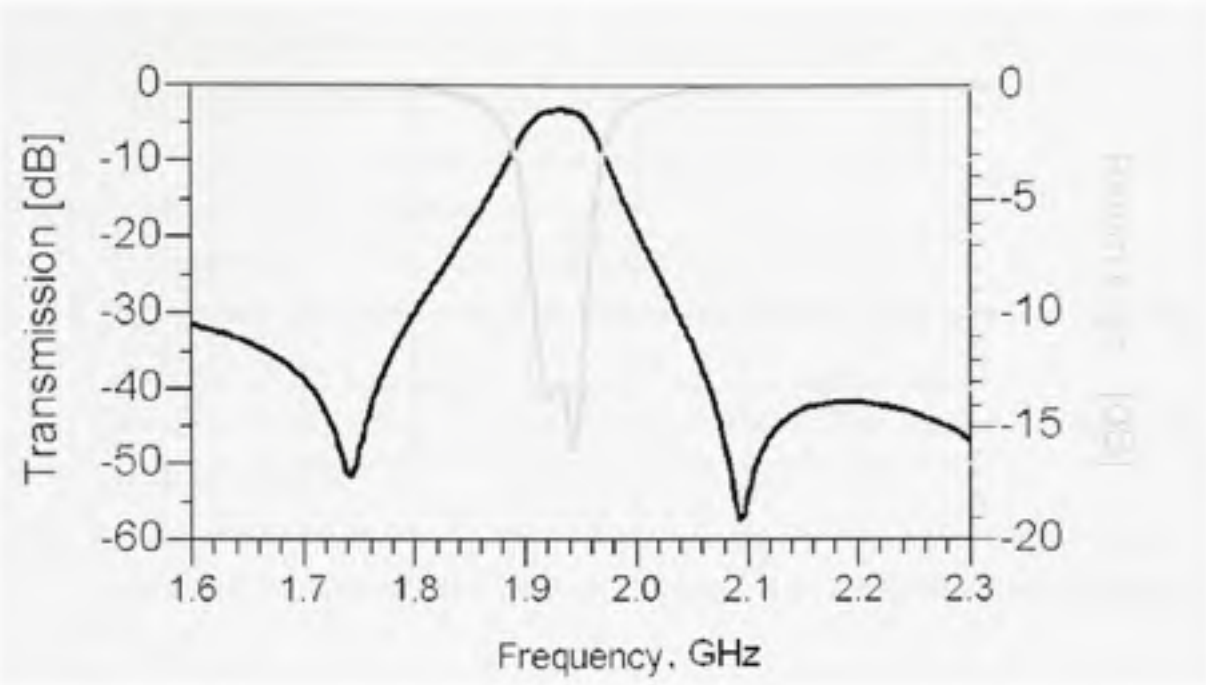

Figure 4.2 ***Electromagnetic simulation results of geometry presented in Figure 4.1.***

Electromagnetic simulation results presented in figure 4.2 show very good attenuation in the reception band and relatively good return loss, these can all be enhanced with further optimisation. Although these preliminary simulation results are satisfactory in themselves as the size of the filter is $0.17\lambda_g$ x$0.06\lambda_g$ which is considerably miniaturised, but when considered in the context of the available space they fall short. Consequently, we considered lumped element filter as a possible option for this technology.

4.3 Design of miniaturised lumped elements filter

In view of the limited space available and the relatively large size of the coupled resonator filter, a different approach was necessary to realise a miniaturised filter. A lumped element approach was chosen as it gives the maximum miniaturization. Although the design of the filter is straightforward, the complexity of the substrate and the fact that stacked vias do not

cover the whole surface between the metal, causing exotic current distribution patterns, have yielded a more complex realisation than originally thought.

The design procedure for the lumped elements filter was as follows:

1. Filter synthesis from the specification using ideal components
2. Using ideal components values to estimate the series resistance of the TrinQuint provided inductors.
3. A finite Q theoretical model using TriQuint component kit of inductors and capacitors is built.
4. A real model was built using transmission lines and TriQuint component kit for each section of the filter and then optimised to approach in performance of the finite Q model
5. Assembly of the different sections of the filter and final optimisation

Each of these steps will be presented briefly in the following sections.

4.3.1 Ideal filter synthesis

An elliptic third order filter was synthesised using Filter Design Guide of ADS. figure 4.3 shows the window where the filter specifications are entered, while figure 4.4 presents the corresponding circuit schematic. It is to be noted that the values for the inductors range between 100 to 500nH, a range that can be realised using the kit provided by TriQuint Semiconductors.

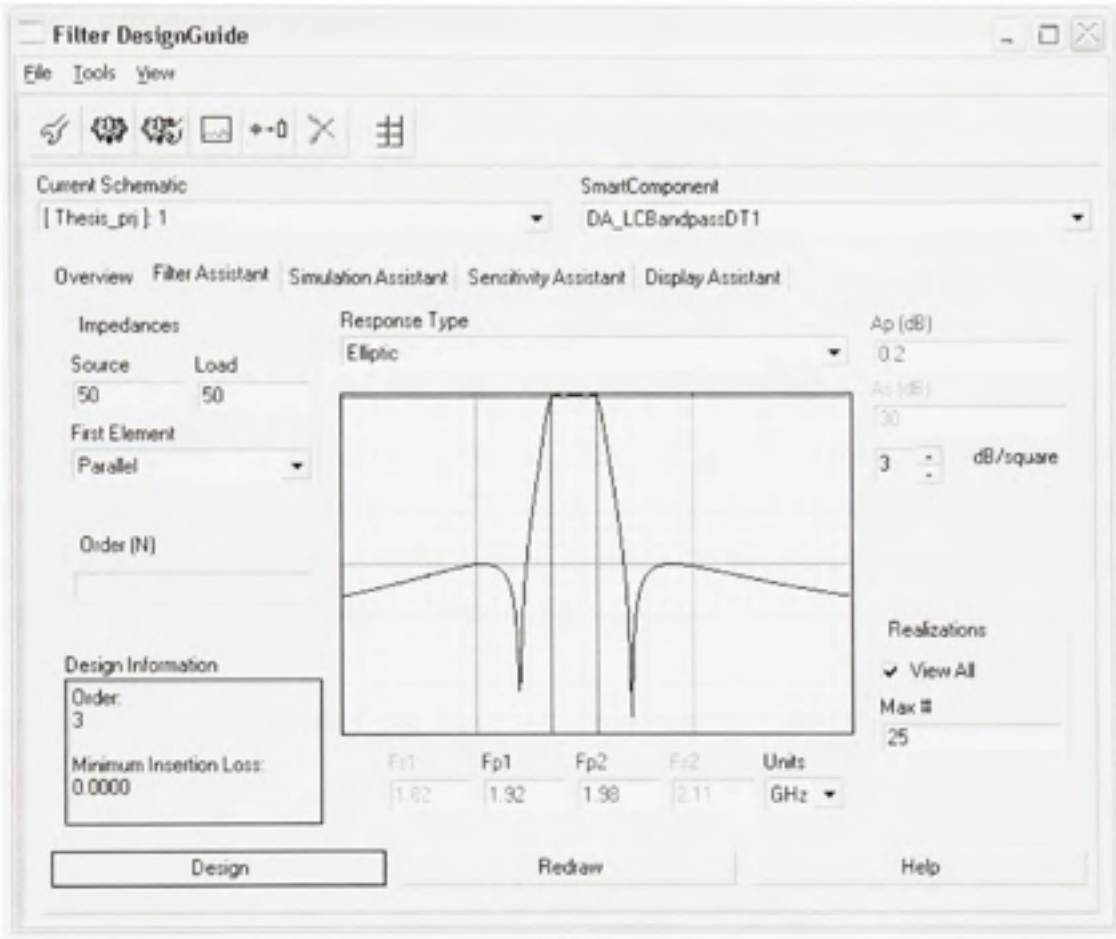

Figure 4.3 ***Filter design guide window.***

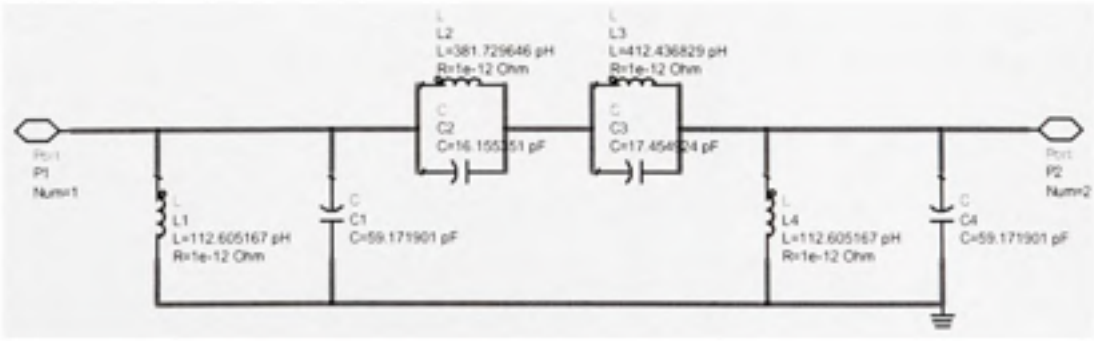

Figure 4.4 ***Synthesised elliptic 3rd. order filter.***

4.3.2 Model with transmission lines

Two models have been constructed: a model using transmission lines that are configured to map to the layers presented in Table 4.1 and the components provided in the TQPED design kit. Another model was constructed using only the components of the design kit, both are illustrated in figure 4.5. The model using transmission lines is optimised to approach in performance that with only lumped components.

An interesting fact, that L1 whose value is 112pH was too low and not realisable using the inductors provided in the design kit. This is likely because of transmission line inductance has larger influence than that of the lumped inductor. This inductor was realised using a short circuited transmission line as illustrated in figure 4.6.

Successively, each section of the filter was optimised in a similar fashion until all the sections were designed.

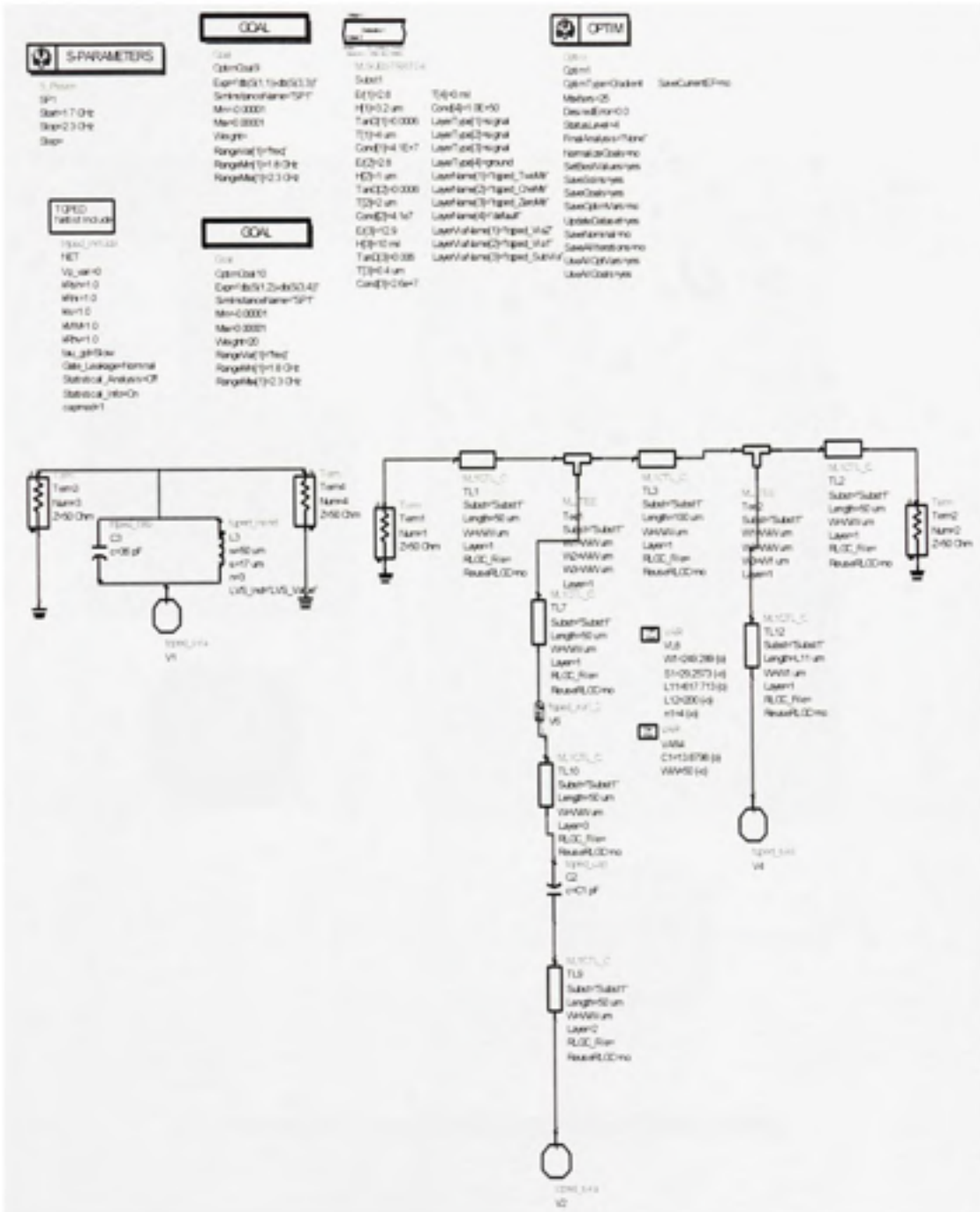

Figure 4.5 ***Optimisation of a filter section including transmission lines Q model.***

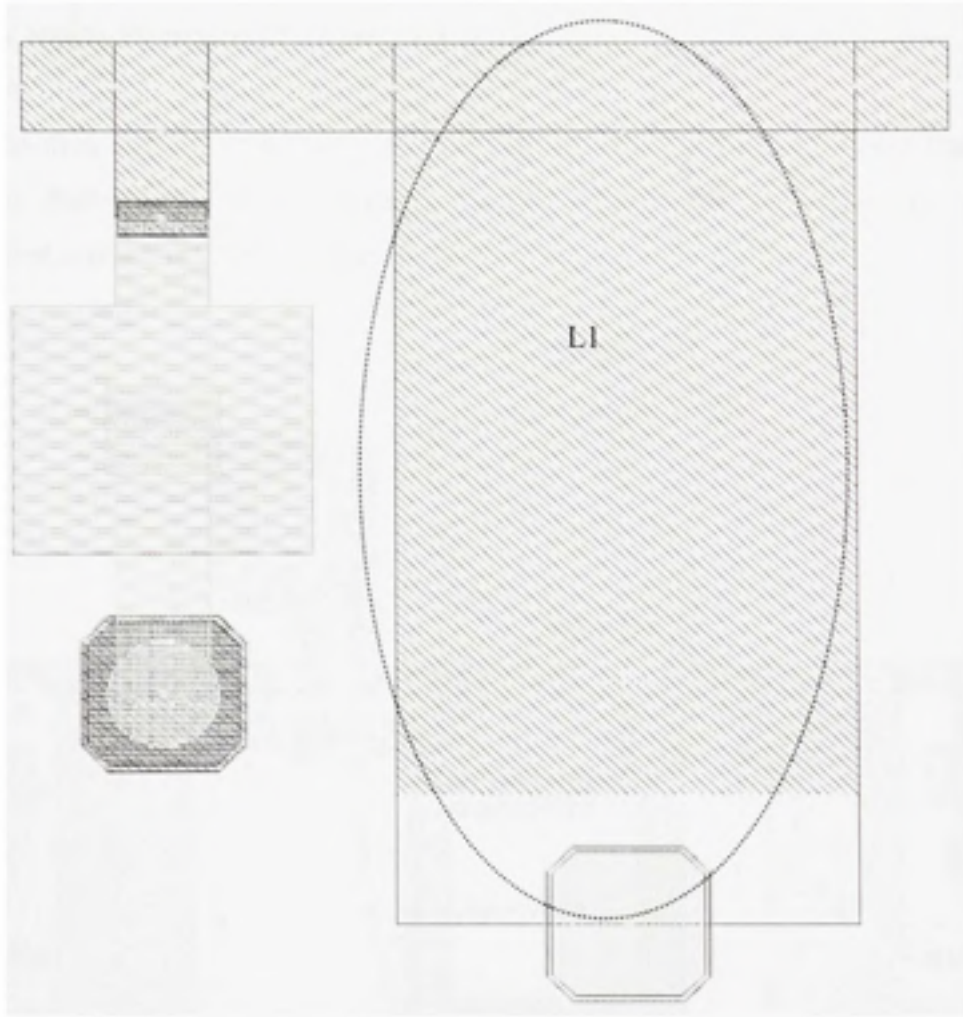

Figure 4.6 ***Layout of an optimised filter section.***

4.3.3 Assembly and final optimisation

The filter sections were assembled in a single layout then circuit optimisation was used to tune the circuit performance. A pair of UMTS filters were designed and their layout and the simulation results are presented in figure 4.7 to figure 4.10

As we note from figures 4.8 and 4.10 the insertion losses are quite high. This is mainly due to the low quality factor of the inductors. A way to overcome these losses is to use Q-compensated active inductors as suggested in [3].

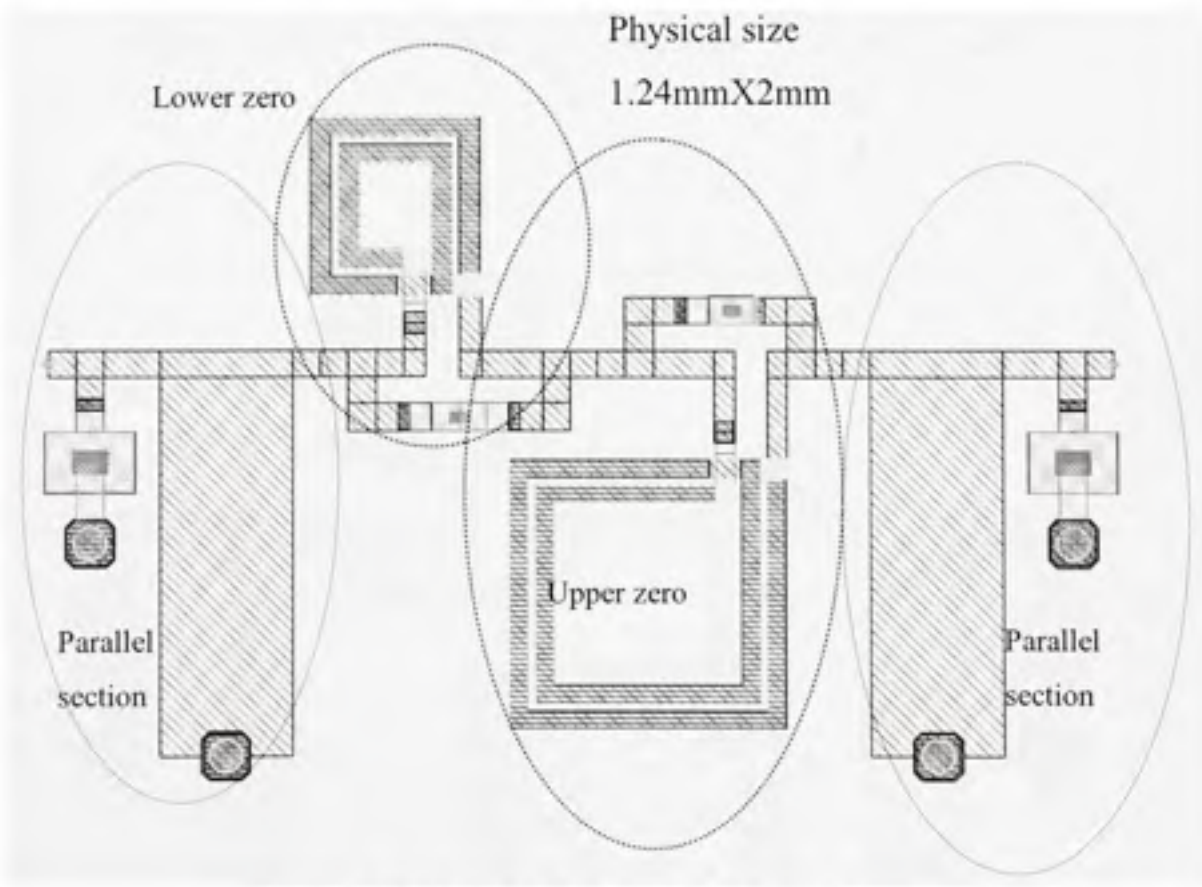

Figure 4.7 ***UMTS Tx band lumped element filter.***

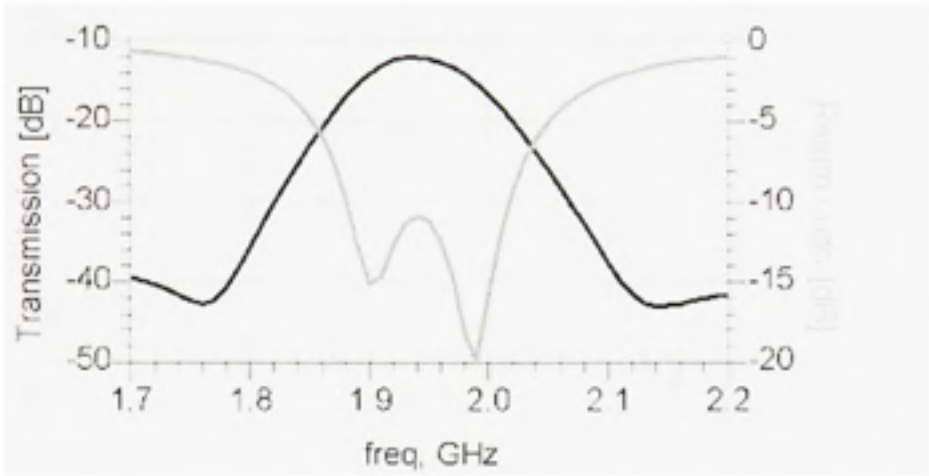

Figure 4.8 ***UMTS Tx band lumped element filter – simulation results.***

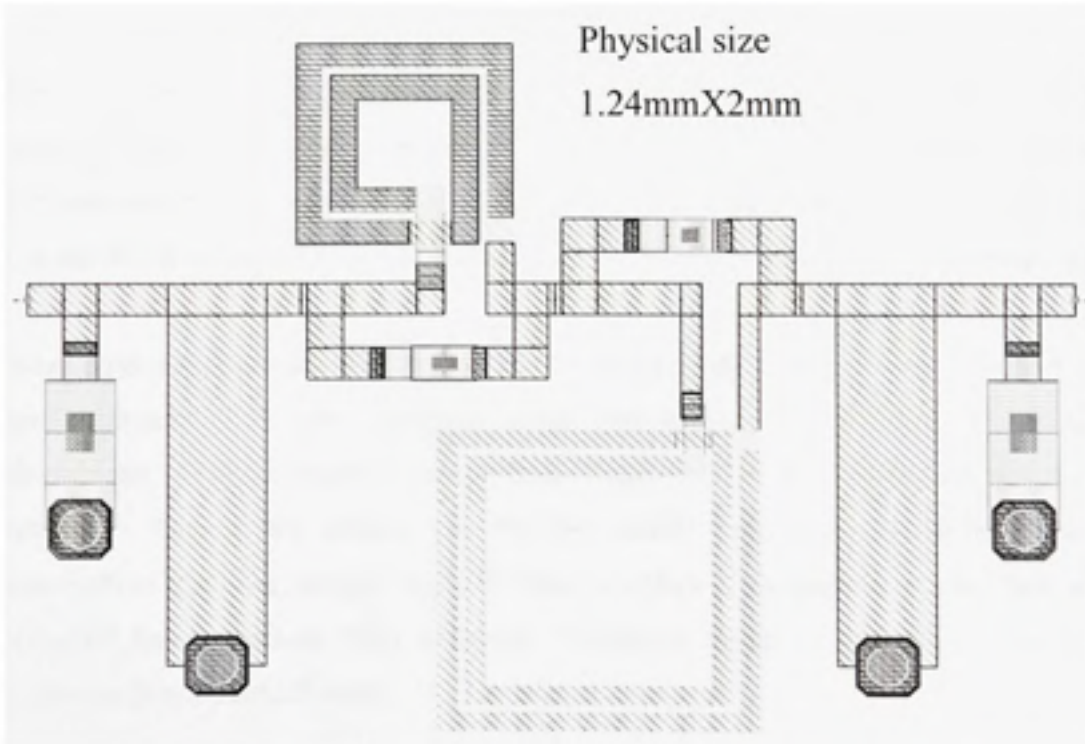

Figure 4.9 ***UMTS Rx band filter.***

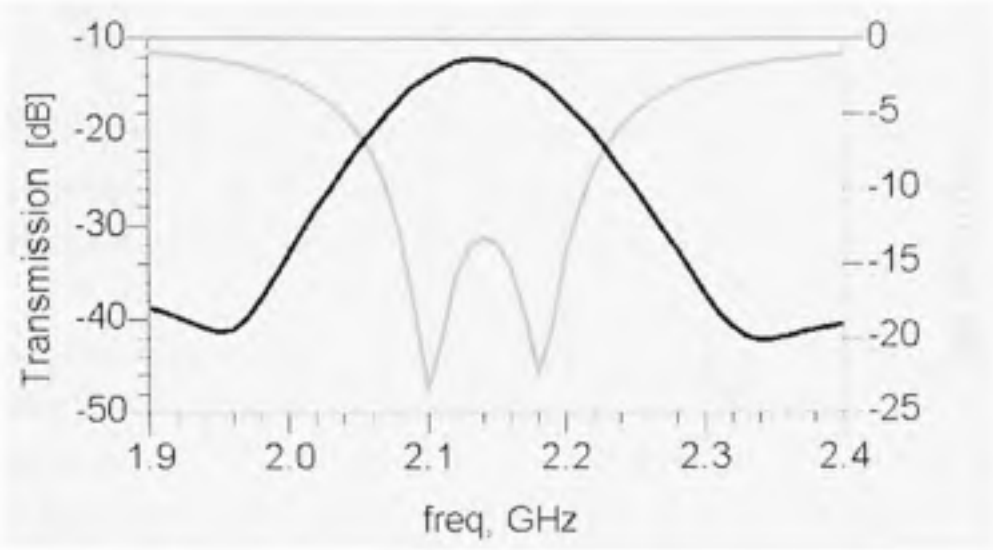

Figure 4.10 ***UMTS Rx band filter – simulation results.***

4.4 Conclusion

In this chapter we have applied the topological optimisation technique to design a coupled resonators filter on a MMIC substrate. The results of the simulations show excellent performance and miniaturisation for the distributed model. While the filter is miniaturised in size, it did not fit the space available for fabrication and thus its fabrication was not pursued.

An alternative approach was then required to further miniaturize the filter. A filter using lumped elements was then designed using the design kit provided by TrinQuint Semiconductor. The simulation results show larger IL than its coupled resonators filter counterpart. Losses are mainly due to low quality factors of inductors. On the miniaturization front the lumped elements filter is orders of magnitude smaller than any of the coupled line resonators filter designed. However, given its limited performance its fabrication was not pursued either.

CONCLUSION

In this thesis we have given an overview of planar filter miniaturization techniques employed in the current state of the art. Further more we have elaborated a methodology for filter miniaturisation based on geometrical optimization.

Using our methodology we have produced a filter structure that provides better performance and smaller size than published results in the open literature. The final topology of the filter was used to realise filters and duplexers on different substrates and technologies with excellent agreement between simulation and measurements. In terms of performance we have been limited by the fabrication processes used, especially on the metal thickness. Naturally, this limitation has resulted in insertion losses that are relatively large but in terms of miniaturization we have managed to reduce the filters and duplexers by 40% compared to what is published in open literature. However, due to the excellent correlation between simulation and measurements obtained throughout our work we have confidence that better insertion losses, as predicted in simulation, can be obtained when proper metallisation is used in fabrication.

Furthermore, we have shown that the design technique of coupled resonator filters can be successfully applied to a MMIC process though the resulting space requirement may be an issue. Still, given its monolithic integration advantage, such a design may yet make to prototyping and may be even production for special applications.

Finally we note that there is more room for miniaturisation using the filter topology we introduced in this work by using multi layer technologies such as LTCC, which can put the size of filters and duplexers within the realm of monolithic integration.

BIBLIOGRAPHY

[1] Aigner, R., *Integration of Bulk Acoustic Wave Filters: Concepts and Trends*, in *MTT-S Digest*. 2004.

[2] Hieng Tiong, S., F. Huang, and M.J. Lancaster, *Highly miniature HTS microwave filters.* Applied Superconductivity, IEEE Transactions on, 2001. **11**(1): p. 349-352.

[3] Kuhn, W.B., F.W. Stephenson, and A. Elshabini-Riad, *A 200 MHz CMOS Q-enhanced LC bandpass filter.* Solid-State Circuits, IEEE Journal of, 1996. **31**(8): p. 1112-1122.

[4] Sagawa, M., K. Takahashi, and M. Makimoto, *Miniaturized hairpin resonator filters and their application to receiver front-end MICs.* Microwave Theory and Techniques, IEEE Transactions on, 1989. **37**(12): p. 1991-1997.

[5] Sheng-Yuan, L. and T. Chih-Ming, *New cross-coupled filter design using improved hairpin resonators.* Microwave Theory and Techniques, IEEE Transactions on, 2000. **48**(12): p. 2482-2490.

[6] Chi-Feng, C., et al., *A miniaturized multilayer quasi-elliptic bandpass filter with aperture-coupled microstrip resonators.* Microwave Theory and Techniques, IEEE Transactions on, 2005. **53**(9): p. 2688-2692.

[7] Hong, J.S. and M.J. Lancaster, *Microstrip filters for RF/microwave applications.* Wiley series in microwave and optical engineering. 2001, New York: Wiley. xii, 471 p.

[8] Goron, E., et al. *Accessing to UMTS filtering specifications using new microstrip miniaturized loop-filters*. in *Microwave Symposium Digest, 2003 IEEE MTT-S International*. 2003.

[9] Cohn, S.B., *Direct-Coupled-Resonator Filters.* Proceedings of the IRE, 1957. **45**(2): p. 187-196.

[10] Cohn, S.B., *Parallel-Coupled Transmission-Line-Resonator Filters.* Microwave Theory and Techniques, IEEE Transactions on, 1958. **6**(2): p. 223-231.

[11] Dishal, M., *Alignment and Adjustment of Synchronously Tuned Multiple-Resonant-Circuit Filters.* Proceedings of the IRE, 1951. **39**(11): p. 1448-1455.

[12] Rizzi, P.A., *Microwave engineering : passive circuits*. 1988, Englewood Cliffs, N.J.: Prentice Hall. xvi, 572 p.

[13] Matthaei, G.L., *Microwave filters : impedance-matching networks, and coupling structures*. 1964, New York: McGraw-Hill. xv, 1096 p.

[14] AgilentTechnologies, *ADS2004A User Manual*. 2005.

[15] Levy, R., *Filters with Single Transmission Zeros at Real or Imaginary Frequencies.* Microwave Theory and Techniques, IEEE Transactions on, 1976. **24**(4): p. 172-181.

[16] Hosoya, K., et al. *A low phase-noise 38-GHz HBT MMIC oscillator utilizing a novel transmission line resonator*. in *Microwave Symposium Digest., 2000 IEEE MTT-S International*. 2000.

[17] Amari, S., et al. *New parallel /spl lambda//2-microstrip line filters with transmission zeros at finite frequencies*. in *Microwave Symposium Digest, 2003 IEEE MTT-S International*. 2003.

[18] Woodin, C., C. Woodin, and M. Goff. *Verification of MMIC on-wafer microstrip TRL calibrationVerification of MMIC on-wafer microstrip TRL calibration*. in *Microwave Symposium Digest, 1990., IEEE MTT-S International*. 1990.

[19] Puglia, K.K., *A general design procedure for bandpass filters dirieved from low pass prototype elements.* Microwave journal, 2001.